REPUBLIC OF TURKEY
YILDIZ TECHNICAL UNIVERSITY
GRADUATE SCHOOL OF NATURAL AND APPLIED SCIENCES

SYNTHESIS OF ENZYME IMMOBILIZED ZEOLITIC IMIDAZOLE FRAMEWORKS AND DETERMINATION OF KINETIC PARAMETERS

GİZEM GÜNER

MSc. THESIS
DEPARTMENT OF CHEMICAL ENGINEERING
PROGRAM OF CHEMICAL ENGINEERING

ADVISER
Assoc. Prof. Dr. DİLEK DURANOĞLU

İSTANBUL, 2019

REPUBLIC OF TURKEY

YILDIZ TECHNICAL UNIVERSITY

GRADUATE SCHOOL OF NATURAL AND APPLIED SCIENCES

SYNTHESIS OF ENZYME IMMOBILIZED ZEOLITIC IMIDAZOLE FRAMEWORKS AND DETERMINATION OF KINETIC PARAMETERS

A thesis submitted by Gizem GÜNER in partial fulfillment of the requirements for the degree of **MASTER OF SCIENCE** is approved by the committee on 02.08.2019 in Department of Chemical Engineering, Chemical Engineering Program.

Thesis Adviser

Assoc. Prof. Dr. Dilek DURANOĞLU

Yıldız Technical University

Approved By the Examining Committee

Assoc. Prof. Dr. Dilek DURANOĞLU

Yıldız Technical University _____

Assoc. Prof. Dr. Emek DERUN, Member

Yıldız Technical University _____

Assoc. Prof. Dr. Rezan DEMİR ÇAKAN, Member

Gebze Technical University _____

This study was partly supported by the BioInterfaces in Technology and Medicine (BIFTM) program of Karlsruhe Institute of Technology (KIT).

ACKNOWLEDGEMENTS

First of all, I would like to express my sincere appreciation to my precious thesis advisor Assoc. Prof. Dr. Dilek DURANOĞLU. She guided me in the best way with her valuable opinions and contributions and patiently guiding me to complete my thesis. She meticulously supported me on this long journey and took care of all my problems during her consultancy.

Next, I would like to express my sincere appreciation to Prof. Dr. Matthias FRANZREB for giving me the opportunity to study at the Karlsruhe Institute of Technology (KIT)/Institute of Functional Interfaces (IFG). He sincerely supported and guided me with his precious opinions during my thesis. I also would like to express my sincere appreciation to Dipl.-Ing. Frank KIRSCHHÖFER and Dr. Gerald BRENNER-WEIß who provided me with every kind of support and followed my experiments with great care and diligence at KIT. They hosted me in Germany in the best way and helped me to complete my experiments with great devotion. Furthermore, I would like to express my sincere gratitude to Dr. Peter WEIDLER, Stefan HEIßLER and Frank FRIEDRICH for their supports to me with their deep knowledges about XRD and FTIR and ESEM analysis, respectively. I would also like to express my sincere thanks to Siegfried HOHMANN and Alexander PUTZ and Barbara SCHMIEG for sharing their valuable views about enzyme kinetics and suggestions by helping me during my laboratory work.

As well, I would like to express my sincere gratitude to dear Anna GRUBER, who welcomed me at her home and helped me to spend my last times in Germany wonderfully. This kind and sweet lady has inspired many students like me and I have no doubt that she will continue to be.

I would like to express my sincere gratitude to dear Seçil AYDIN, who supported me with her valuable views about synthesis of ZIFs. I would also like to thank dear Gizem UZUN for supporting and encouraging me throughout this work.

Finally, I would like to express my sincere gratitude to my dear mother Serpil GÜNER, my dear father Yücel GÜNER and my little brother Yiğit GÜNER who made the greatest effort for me to come to these days. As well, I would like to express my gratitude with love to my dear Barış DİLER who has always supported me, encouraged me and helped me to discover myself at every stage of my thesis. His love gave me the power to continue in my darkest times, and he's now one of my family. I dedicate my thesis to my beloved family who has always been with me.

August, 2019

Gizem GÜNER

TABLE OF CONTENTS

Page

LIST OF SYMBOLS viii

LIST OF ABBREVIATIONS ix

LIST OF FIGURES x

LIST OF TABLES xii

ABSTRACT xiii

ÖZET xiv

CHAPTER 1

INTRODUCTION 1

1.1 Literature Review 1

1.2 Objective of the Thesis 4

1.3 Hypothesis 4

CHAPTER 2

METAL ORGANIC FRAMEWORKS (MOFS) AND ENZYMES 5

2.1 Metal Organic Frameworks (MOFs) 5

2.1.1 History of MOFs 6

2.1.2 Structure of MOFs 6

2.1.3 Purification and Activation of MOFs 7

2.1.4 Methods of MOF Synthesis 8

2.1.5 Applications of MOFs 14

2.1.6 Zeolitic Imidazolate Frameworks (ZIFs) 15

2.1.7 Characterization Techniques 19

2.2 Enzymes 21

2.2.1 Enzyme Immobilization 22
2.2.2 Horseradish Peroxidase Enzyme 26
2.2.3 Enzyme Kinetics 28

CHAPTER 3

EXPERIMENTAL STUDIES 31
3.1 Chemical Materials 31
3.2 Devices 31
3.3 ZIF-90 Synthesis with Non-Solvothermal Technique 32
3.4 ZIF-8 Synthesis with Non-Solvothermal Technique 32
3.5 Enzyme Immobilization into ZIFs 34
3.6 Chracterization of ZIFs and Enzyme Immobilized ZIFs 34
3.6.1 X-Ray Diffraction Analysis (XRD) 34
3.6.2 ESEM and EDX Analysis 34
3.6.3 FTIR Analysis 35
3.7 Determination of Enzyme Loading into ZIF samples 35
3.7.1 Anaylsis of HRP 36
3.8 Determination of Kinetic Parameters 36

CHAPTER 4

RESULTS AND DISCUSSION 38
4.1 Energy Dispersive X-Ray (EDX) Results 38
4.2 Effect of PVP Concentration 40
4.3 Effect of Molar Ratios 42
4.5 HRP Immobilization 44
4.5.3 HRP Loading into ZIF Samples 47
4.6 Enzyme Kinetics Results 47

CHAPTER 5

CONCLUSION 50
REFERENCES 52

APPENDIX-A

SYNTHESIS CONDITIONS OF ZIF SAMPLES 55

APPENDIX-B

ABSORBANCE VALUES AT DIFFERENT ABTS CONCENTRATIONS 57

APPENDIX-C

CALIBRATION CURVES..... 59

APPENDIX-D

PRODUCT CONCENTRATION - TIME GRAPHS..... 60

CURRICULUM VITAE..... 62

LIST OF SYMBOLS

A2	Organic substrate
AH2	Aromatic substrate
E	Enzyme
E_f	Enzyme concentration of final solution
E_i	Enzyme concentration of initial solution
ES	Enzyme-substrate complex
E_T	Total enzyme concentration
E_w	Enzyme concentration of washing solution
k	Specific rate constant
k_{cat}	Turnover number
K_m	Michaelis-Menten constant
L_{enzyme}	Enzyme Loading
M	Molecular weight
N	Avogadro's number
P	Product
S	Substrate
T	Temperature
V_f	Volume of final enzyme solution
V_i	Volume of initial enzyme solution
V_{max}	Maximum velocity
V_w	Volume of washing enzyme solution

LIST OF ABBREVIATIONS

ABTS	2,2′-azino-di-(3-ethylbenzothiazoline sulfonic acid)
BCA	Bicinchoninic Acid
BSA	Bovine Serum Albumin
CAT	Catalase enzyme
DCC	N,N’-dicyclohexylcarbodiimide
EDC	1-ethyl-3-(3-dimethylaminopropyl) carbodiimide
EDX	Energy Dispersive X-Ray
ESEM	Environmental Scanning Electron Microscope
FPS	Fluorescence Polarization Spectroscopy
FTIR	Fourier Transform Infrared Spectroscopy
HmIm	2-Methylimidazole
HRP	Horseradish Peroxidase
ICA	2-Imidazolecarboxaldehyde
IUPAC	International Union of Pure Applied Chemistry
MIL	Materials of Institute Lavoisier
MOF	Metal Organic Framework
PBS	Phosphate Buffered Saline
PSM	Post-Synthetic Modification
PVP	Polyvinylpyrrolidone
SBP	Soybean Peroxidase
SEM	Scanning Electron Microscopy
TEM	Transmission Electron Microscopy
TP	Turnip Peroxidase
XRD	X-Ray Diffraction
ZIF	Zeolitic Imidazole Framework

LIST OF FIGURES

Page

Figure 2. 1 Synthesis of one dimensional, two dimensional and three dimensional metal organic frameworks 5
Figure 2. 2 Conventional solvothermal synthesis of MOF structures 10
Figure 2. 3 Microwave-assisted MOF synthesis 12
Figure 2. 4 Sonochemical synthesis of MOFs 12
Figure 2. 5 Electrochemical MOF synthesis 13
Figure 2. 6 Mechanochemical MOF synthesis 14
Figure 2. 7 Examples of ZIFs classified by topology 16
Figure 2. 8 Structure of ZIF-90 17
Figure 2. 9 Formation scheme of ZIF-90 17
Figure 2. 10 Formation scheme of ZIF-8 18
Figure 2. 11 Structure of ZIF-8 18
Figure 2. 12 Crystal growth evolution of ZIF-8 over time. 19
Figure 2. 13 Comparison of experimental result to simulated pattern from known ZIF-8 pattern 20
Figure 2. 14 De Novo approach and structural confinement 26
Figure 4. 1 ESEM image of R90 38
Figure 4. 2 ESEM image of R8-2 39
Figure 4. 3 XRD patterns of ZIF-90 samples at different PVP concentrations 40
Figure 4. 4 ESEM images of (a) R90 and (b) R90-2 41
Figure 4. 6 XRD patterns of ZIF-8 samples at different molar ratios 43
Figure 4. 7 ESEM images of (a) R8-2 and (b) R8-025 samples 43
Figure 4. 8 FTIR spectrum of HRP immobilized ZIF-90 samples 44
Figure 4. 9 XRD patterns of HRP immobilized ZIF-90 samples 45
Figure 4. 10 FTIR spectrum of HRP immobilized ZIF-8 samples 45
Figure 4. 11 XRD patterns of HRP immobilized ZIF-8 samples 46

(a) R90-2H10 48
(b) R8-025H10 48
Figure 4. 12 Michealis-Menten plots for (a) R90-2H10 and (b) R8-025H10 HRP-ZIF samples 48
Figure B. 1 Absorbance values for R90-2H10 at different initial ABTS concentrations 57
Figure B. 2 Absorbance values for R8-025H10 with different ABTS concentrations 58
Figure C. 1 Calibration curve for R90-2H10 59
Figure C. 2 Calibration curve for R8-025H10 59
Figure D. 1 Product concentration against time plot for R90-2H10 60
Figure D. 2 Product concentration against time plot for R8-025H10 61

LIST OF TABLES

Page

Table 2. 1 Methods used in the synthesis of MOFs 8

Table 2. 2 The topologies of some ZIFs and also metal and inorganic linkers 15

Table 2. 3 Classification of plant peroxidases 27

Table 3. 1 Materials list for ZIF and HRP encapsulated ZIF samples 31

Table 3. 2 Codes for ZIF samples and HRP encapsulated ZIF samples 34

Table 4. 1 Corresponding EDX element mapping of R90 39

Table 4. 2 Corresponding EDX element mapping of R8-2 40

Table 4. 3 Encapsulation efficiencies, HRP loading and yield of HRP-ZIF composites 47

Table 4. 4 Michealis-Menten kinetic parameters, k_{cat} and enzyme efficiency values with the literature data 49

Table A. 1 The amount of starting materials used for synthesis of ZIF-90 samples and HRP-ZIF-90 composites 55

Table A. 2 The amount of starting materials used for synthesis of ZIF-8 samples and HRP-ZIF-8 composites 56

ABSTRACT

SYNTHESIS OF ENZYME IMMOBILIZED ZEOLITIC IMIDAZOLE FRAMEWORKS AND DETERMINATION OF KINETIC PARAMETERS

Gizem GÜNER

Department of Chemical Engineering

MSc. Thesis

Adviser: Assoc. Prof. Dr. Dilek DURANOĞLU

Zeolitic imidazole frameworks (ZIF), which are type of metal organic frameworks (MOF), were succesfully synthesized with non-solvothermal technique at room temperature. First, the ZIF-8 and ZIF-90 structures were synthesized at different conditions, X-ray diffraction (XRD), Environmental Scanning Electron Microscopy (ESEM), Energy Dispersive X-Ray (EDX), Fourier Transform Infrared Spectroscopy (FTIR) analyses were used in order to determine the optimum conditions for the desired ZIF characteristics.

ZIF-90 and ZIF-8 crystal structures were preserved after immobilization of the Horseradish Peroxidase (HRP) enzyme. Higher amount of HRP was encapsulated into ZIF-90 samples than ZIF-8 samples, moreover, obtained yield was higher in the case of ZIF-90. HRP encapsulated ZIF composites were used for the further enzyme kinetic studies in ABTS (2,2′-azino-di-(3-ethylbenzothiazoline sulfonic acid) oxidation reaction. Compared to ZIF-8, higher reaction rate was obtained with the prepared HRP encapsulated ZIF-90 sample. Moreover, enzyme efficiency of prepared HRP encapsulated ZIF-90 sample was significantly higher than prepared HRP encapsulated ZIF-8 sample. Prepared HRP encapsulated ZIF-90 sample in our study showed better enzyme efficiency than free HRP enzyme.

Key words: Metal organic framework, zeolitic imidazolate framework, enzyme immobilization, horseradish peroxidase, Michaelis-Menten equation

ENZİM İMMOBİLİZE EDİLMİŞ ZEOLİTİK İMİDAZOL KAFES YAPISININ SENTEZİ VE KİNETİK PARAMETRELERİN BELİRLENMESİ

Gizem GÜNER

Kimya Mühendisliği Anabilim Dalı

Yüksek Lisans Tezi

Tez Danışmanı: Doç. Dr. Dilek DURANOĞLU

Metal organik çerçevelerin (MOF) bir türü olan Zeolitik imidazol çerçeveler (ZIF), oda sıcaklığında solvotermal olmayan teknik ile başarıyla sentezlenmiştir. İlk olarak, ZIF-8 ve ZIF-90 yapıları farklı koşullar altında sentezlenmiş, X-ışını kırınımı (XRD), Çevresel Taramalı Elektron Mikroskobu (ESEM), Enerji Dağıtıcı X-Işını (EDX), Fourier Dönüşüm Kızılötesi Spektroskopisi (FTIR) analizleri kullanılarak arzu edilen ZIF özellikleri için optimum koşullar belirlenmiştir.

Horseradish Peroxidase (HRP) enziminin immobilizasyonundan sonra ZIF-90 ve ZIF-8 kristal yapıları korunmuştur. ZIF-90 numunelerine ZIF-8 numunelerine göre daha yüksek miktarda HRP enkapsüle edilmiştir, ayrıca ZIF-90 numuneleri için elde edilen verim daha yüksektir. HRP enkapsüle edilmiş ZIF kompozitleri, ABTS (2,2′-azino-di-(3-etilbenzotiyazolin sülfonik asit) oksidasyon reaksiyonunda kullanışmış ve kinetik açıdan incelenmiştir. Hazırlanan ZIF-90 numuneleri ile ZIF-8 numunelerine kıyasla daha yüksek reaksiyon hızı elde edilmiştir. HRP enkapsüle edilmiş ZIF-90 numunesinin enzim etkinliği, hazırlanan HRP enkapsüle edilmiş ZIF-8 numunesinden çok daha yüksektir. Ayrıca çalışmamızda hazırlanan ZIF-90 numunesi serbest HRP enzimine göre daha iyi enzim etkinliği göstermiştir.

Anahtar Kelimeler: Metal organik çerçeve, zeolitik imidazolat çerçeve, enzim immobilizasyonu, yabanturbu peroksidaz enzimi, Michaelis-Menten denklemi

CHAPTER 1

INTRODUCTION

1.1 Literature Review

From past to present, the nature has been examined and investigated by the mankind in order to find answers and solutions of some of the complicated problems in life such as aerodynamics, self-healing, catalysis and energy collection [1]. For that reason, surely, one of the most significant biomacromolecules for mimicking the life is enzyme [2].

Enzymes are originated in linear series of amino acids that composes complex structures with highly specific catalytically active sites [1]. Enzymes are accepted as easy-productive and are used in many large-scale processes of biosciences and biotechnology such as pharmaceutical production, biofuel production, food processing, agricultural feeds, polymer synthesis and paper industry [3].

Although enzymes have high catalytic activity, green chemistry conditions, high reaction specificity and many areas of usage in several processes, there are some problems and challenges that science world faces to maintain the stability and activity of enzymes. For instance, one of the examples of these challenges is the catalytic activity loss of free enzyme as the reaction proceeds. In addition, stability of aqueous solutions of free enzymes is one of the most critical points that can inhibit the use of enzymes in different applications. These kinds of problems can be come through by several processes and strongest one of these methods is the enzyme immobilization which generates an outstanding groundwork for enhancing the utility of the enzyme [4].

Immobilization process is stabilization of enzyme to a phase of a distinct support or matrix which allows the exchange of medium containing substrate molecules and maintains the biological functions of enzymes under various reaction conditions [5]. It is reported in several researches that immobilized enzymes present higher stability, more increased functional efficiency, more continuous usage of enzyme, higher enzyme

and substrate ratio than free enzymes [4]. Many biological techniques are available to immobilize enzymes such as metal organic frameworks. [5].

Metal ions and organic linkers are composed and formed a crystalline structure (one-to-two and three-dimensional) named metal organic frameworks (MOFs) [6]. For the synthesis of the liquid phase MOF, the solvent is added onto solid metal salt and the organic ligand, or the metal salt and the ligand solutions are mixed with each other. The synthesis methods of MOFs can be divided into two methods: traditional and alternative. Traditional methods are reviewed under two headings as solvothermal and non-solvothermal methods while alternative methods are microwave-assisted synthesis, sonochemical synthesis, electrochemical synthesis and mechanochemical synthesis [7]. Comparing the other synthesis methods, the non-solvothermal method is very easy and low cost synthesis method of MOFs due to the fact that high temperature and high pressure are not required for this process. Certain well-known MOFs like ZIF-8 and ZIF-90 can be synthesized by non-solvothermal method in a short time at room temperature by mixing only the starting materials [8].

MOFs have many strong properties for enzyme immobilization such as high thermal and mechanical stability, high surface area and pore size, configurable crystal morphology and chemical composition [9]. Usually, there are four main methods that are examined for obtaining MOF-enzyme bio-composites: surface attachment, covalent binding, pore encapsulation and incorporation de Novo. Among these four methods, encapsulation is one of the most effective ones in order to prevent enzyme from physical enzyme denaturation against heating, dehydration, ionic strength of solution and prevent enzyme deactivation caused by aggregation [1].

Enzyme kinetics, which is figured out by the estimation of the equilibrium between enzyme, substrate, enzyme-substrate complex and product, is required to be known due to the understanding of the immobilization of enzyme into MOF and a reaction between enzyme-MOF complex and a certain substrate. After several calculations, Michaelis-Menten equation is obtained and used for the estimation the velocity of the enzymatic reaction. V_{max} and K_m constants obtained from Michaelis-Menten equation are determinative for evaluating the rate of the reaction and the activity of the enzyme. K_m, which is Michaelis-Menten constant, equals to the substrate concentration when the velocity is half of maximum velocity (V_{max}) and represents the rate at maximum velocity by means that high K_m means a slow rate [10].

Liao et al. (2017) demonstrated that the enzymes preserve their biological function under denaturing situations afterwards being encapsulated in MOF crystals via a de Novo approach. This improved stability originates from encapsulation of the enzyme molecules in the mesoporous cavities in the MOFs while decreasing the structural mobility. They used catalase (CAT) as an encapsulated enzyme into zeolitic imidazolate frameworks (ZIF-90 and ZIF-8). Embedded CAT and free CAT are exposed to a denaturing reagent as urea and high temperatures (80 °C). Results showed that the encapsulated CAT maintains its biological functions under the denaturing conditions even existence of hydrogen peroxide. On the other hand, free CAT′s activity is undeterminable. Fluorescence spectroscopy indicated that structure of the embedded CAT was affected less than free CAT under denaturing conditions. Free CAT and CAT at ZIF were exposed to urea. Urea caused the deterioration of hydrophobic reactions due to the fact that water molecules form a compound with nonpolar groups in the protein. This caused the protein to dissipate and lose its biological function. CAT-ZIF has been confirmed to be stable prior to catalytic testing and spectroscopy [5].

Cravillon et al. (2012) investigated the synthesis of ZIF-8 at room temperature. They were able to synthesize monodisperse pure ZIF-8 without using any stabilizing ligand or activation (conventional heating, microwave or ultrasound radiation) method. 1:8:700 Zn:2-MeIM:MeOH in excess of 2-MeIM and methanol as solvent were used for synthesis of ZIF-8. The ZIF-8 structure synthesized in the nano scale was observed to be stable up to ~ 200 °C, while the micro-scale structure was stable up to ~ 400 ° C. [32].

Doonan et al. (2017) synthesized a ZIF-90 which was consisting of an aldehyde functional group in the 2-position of the imidazole unit. It could be converted into an alcohol group by one step synthesis. The resulting structure had high thermal and solvent stability [14].

Liao et al. (2017) used chemical agents to test de Novo encapsulation method. Encapsulated enzymes were exposed to chemical agents. After this step, they examined the resultant catalytic activity of enzymes by fluorescence spectroscopy. The results demonstrated that the encapsulation ensured by the de Novo approach keeps enzymes functional under wider range of reaction statements and decrease the structural changes [5].

1.2 Objective of the Thesis

Synthesis of metal organic frameworks (MOF) for enzyme immobilization applications were aimed in this study. For this purpose, zeolitic imidazolate frameworks (ZIF), a type of MOFs, were synthesized with non-solvothermal technique at room temperature. Effect of metal/organic molar ratio were investigated, and prepared ZIFs and enzyme-ZIF composites were characterized. In addition, Michaelis-Menten enzyme kinetic parameters were determined.

1.3 Hypothesis

Enzyme immobilization are carried out in order to increase the enzyme stability and to prevent catalytic activity losses of free enzymes. Metal Organic Frameworks could be a good candidate for enzyme immobilization, due to their high surface area, adjustable pore size, crystal morphology and chemical composition. Particularly, mesoporous MOFs are very attractive for enzyme immobilization due to the high pore volume and free space, which improves the stability and provides selectivity for specific substrates. The use of organic solvents in immobilization processes may deactivate or block some regions of the enzyme. However, water, an environmentally friendly solvent, can be used as a solvent during the preparation of the enzyme-MOF composites. MOFs and enzyme-MOF composites can be prepared by using non-solvothermal method at room temperature.

CHAPTER 2

METAL ORGANIC FRAMEWORKS (MOFs) and ENZYMES

2.1 Metal Organic Frameworks (MOFs)

Metal organic frameworks (MOFs) are crystalline structures composed by a combination of metal ions and organic linkers [6]. MOFs, which can be one-to-two, three-dimensional, have an extremely high surface area (beyond 6000 m^2/g), adjustable pore size and function, controllable crystal morphology and tunable chemical compositions. In addition, MOFs have high thermal and mechanical stability and good opto-electronic properties [9]. It can be seen 1D, 2D and 3D networks of metal organic frameworks, respectively (Figure 2.1).

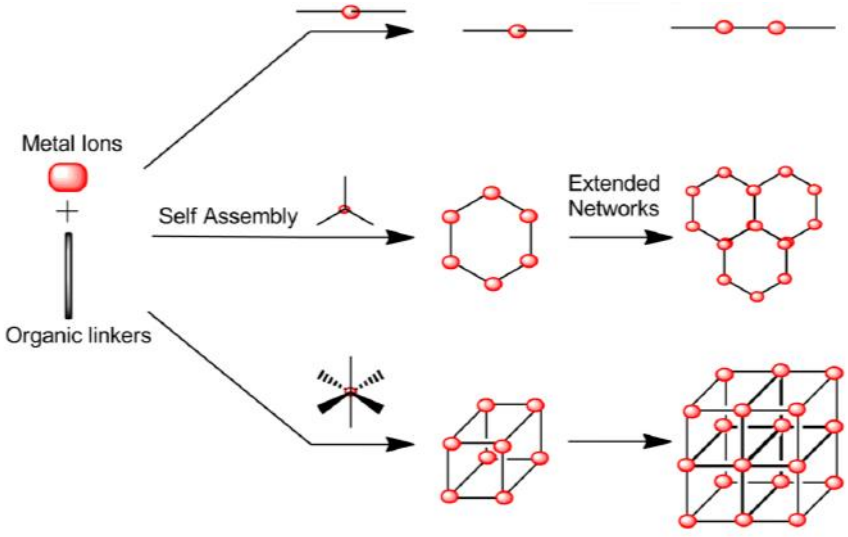


Figure 2.1 Synthesis of one dimensional, two dimensional and three dimensional metal organic frameworks [8]

They can host many molecules due to their porous structure [11]. They can possess ultrahigh porosity up to 90% free volume [9]. Based upon their superior properties,

MOFs are very suitable for many applications [6]. They are also excellent potential supports for enzyme immobilization [2].

2.1.1 History of MOFs

Metal organic frameworks first appeared in a declaration about the chemistry of polymers in the 1960s. The term was first used by Yaghi and Li in 1995. In 1999, Yaghi et al. illuminated the MOF structure called MOF-5. Williams et al. (1999) found the MOF called HKUST-1. After that, Férey et al. studied out the Materials of Institute Lavoisier (MILs). In 2006, Férey et al.'s work on the MIL-101 revealed that the chemical structure could be understood by targeted chemistry and global optimization studies [12].

Chemically stable metal organic framework structures with zinc imidazole-based networks (ZIF-1, 4, 6, 8, 10, 11) were introduced by Yaghi in 2006. According to the report, the chemical structure of ZIF-8 had not changed for 7 days even after boiling in water, methanol and benzene solutions. It was noted that it also remained stable for 24 hours in sodium hydroxide solution. In 2008, MOF called UiO-66 was added to the metal organic frame types by Lillerud's group. Many different types of this material have been discovered throughout the years [12].

Studies in the MOF area have been made mainly on transition-metal based materials, while the main group metal-based networks are less researched. Recently, porous coordination polymers consisting of Li and Mg have attracted great attention due to high gas adsorption properties. Studies have revealed that these materials showed promising results in gas adsorption, but the correct synthesis of these materials is still under investigation. A new metal organic framework structure chemistry discipline has been established through the work done on the metal organic frames produced so far. With this knowledge, MOF applications can be carried out in large scale industrial systems [12].

2.1.2 Structure of MOFs

Metal organic frames are crystalline porous coordination polymers consisting of organic ligands (for example terephthalate, carboxylate or imidazole derivatives) and metal ions or aggregates. These complex materials were identified by IUPAC (International Union of Pure Applied Chemistry) as coordination networks with organic ligands including

potential gaps in 2013. The structures of these materials vary based on the environmental conditions. Inorganic component of network composed by metal consists of clusters that come together from the center and anions which provide polyhedral forming or the rare earth (scandium), p block (aluminium) and transition (zinc, iron, copper) elements [12].

The pore size, particle shape, the frame topology, and the overall chemical function of the structure are all influenced by the choice of metal ion and organic ligand. It is possible to add functionality to the MOF structure during synthesis or after synthesis by post-synthetic modification (PSM) reactions. With these modifications, MOFs can be used in special applications by providing properties such as magnetization, luminescence and chirality [8].

A good definition of the synthesis conditions with the selection of the correct organic and inorganic variables allows the formation of bonds with the intended properties [12].

The complication of the MOF bonds can be compared to the protein structure in which the macromolecule is identified at four varied levels as primary, secondary, tertiary and quaternary structures. In this way, it can be understood how each unit of MOF networks come together and how this relationship affects MOF characteristics [12].

2.1.3 Purification and Activation of MOFs

Purification and activation of MOFs are very important steps, especially for post-synthetic processes. The impurity caused by the by-products in the reaction of catalytic applications can imitate the catalyst and significantly disrupt the possibility of absorption. Purification is a process, frequently carried out at high temperatures with a solvent. Activation is a more complicated process requiring pore emptying. If the guest molecule and the frame structure are connected by strong bonds or if the removal requires very high temperatures, removing the additives from the porous structure with the help of heat may cause the frame to collapse. Therefore, the activation process is a difficult process that requires attention. Different methods can be used to facilitate activation of MOFs. The most common of these methods is to choose a volatile solvent. Volatile solvents allow the process temperature to be reduced [7].

2.1.4 Methods of MOF Synthesis

The methods of synthesis of MOF could be categorized into two types as traditional methods and alternative methods [7]. Table 2.1 shows a summary of these methods. The liquid phase synthesis in which the separate metal salt and ligand solutions are mixed together or the solvent addition onto the solid metal salt and ligand in the reaction flask, is commonly used as the synthesis of MOF. Solvent selection is important in specifying the thermodynamic and activation energy for a given reaction [11]. Water and organic solvents (such as DMF) fill the pores together with unreacted residues of the starting compounds. Dense structures are known to be more stable thermodynamically [7]. Solid phase synthesis is also used as a production method because it is faster and easier. However, this method has difficulties in the determination of product structure and single crystal yield [11].

Table 2. 1 Methods used in the synthesis of MOFs [7]

Synthesis Methods	Time	Temperature
Solvothermal	48-96 hours	353-453 K
Non-Solvothermal	5 min-2 hours	298-310 K
Electrochemical	10-30 minutes	373-303 K
Mechanochemical	30 min-2 hours	298 K
Slow Evaporation	7 days-7 months	298 K
Sonochemical	30-180 min	273-313 K
Microwave	4 min-4 hours	303-373 K

Slow evaporation method is a recently used method for the production of MOF crystals [11].

In the MOF and ZIF synthesis process, it is important to pay attention to the generation of inorganic building blocks without deteriorating the chemical structure which is thermally and chemically sensitive. At the same time, nucleation and crystallization must take place in order to formation of the framework structure in the correct phase. MOF production methods can be optimized to meet these requirements. As a result of the researches on the synthesis of MOF, it has been found that MOFs synthesized by different methods using same reagents can represent different morphologies, particle shapes, particle sizes and particle distribution. The alteration of the parameters such as concentration of the reagents, the order of addition, the concentration of the solvent, pH, the agitation of the reaction mixture throughout the reaction, addition of the variable

ligands and the reaction time may have considerable effects in the structure or morphology of the formed particles. For instance, the increased reaction temperature produces more intense structures. The properties of the particles are affected by these differences in MOFs and provide the usage of MOFs in different areas. For example, sonochemical or microwave-assisted production methods may be preferred because of the need for small particles for membrane formation. In order to produce thin films, spheres, membranes, nanoparticles, microfibers and monolayers, different morphologies and types of structures are needed, such as crystal size and shape, all of which require different synthetic methods. In addition, the conversion of the pore size of MOFs from the micropores to the larger pores and mesopores changes the capability of MOFs to intake or demobilize molecules, as well as host-guest interactions within the framework structure [8].

2.1.4.1 Traditional Methods

Traditional methods can be investigated under two headings as solvothermal and non-solvothermal methods. The term solvothermal refers to the utilization of solvents. In the case of solvothermal methods, the reaction proceeds at the boiling point of the solvent or above the boiling point in closed chemical reactors. In such systems, solution vapor or pump can cause high pressure. On the other hand, in non-solvothermal systems, the reaction occurs at atmospheric pressure and below the solvent boiling point [7].

Solvothermal reactions are the reactions which are carried out at temperatures at the boiling point of the solvent in autogenous closed containers. The initiative materials in solvothermal synthesis may go through unforseen chemical changes, usually containing high boiling point solvents (ethanol, methanol, dimethyl formamide, diethyl formamide, acetonitrile, acetone). Under these circumstances, nanoscale morphologies, which are not usually observed in conventional methods can occur. Solvent mixtures may be used to prevent problems that may arise from different solubility of different starting materials [11].

Figure 2.2 illustrates the schematic diagram of the conventional solvothermal MOF synthesis method.

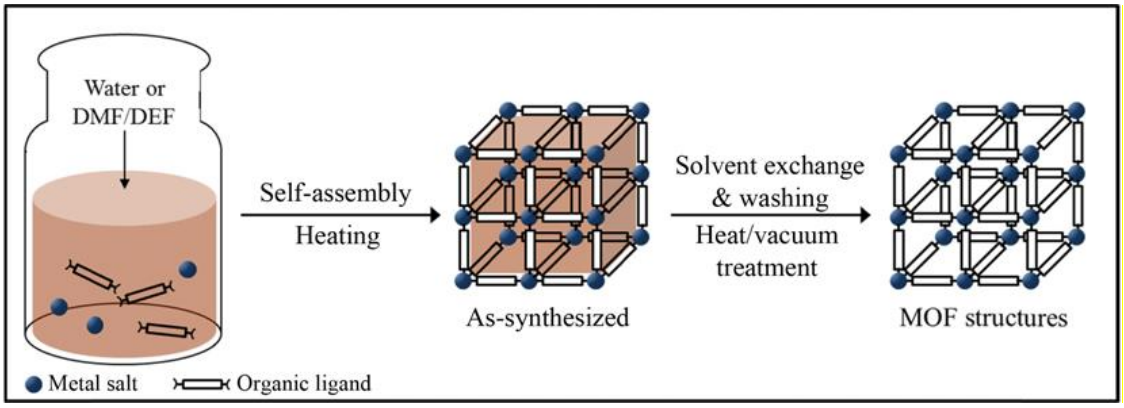


Figure 2. 2 Conventional solvothermal synthesis of MOF structures [13]

In solvothermal synthesis which can be carried out at different temperatures, the product has a high crystallinity and yield. Heating the solvent to above of its boiling point at 1 atm pressure, causes the solubility of the salts formed during the reaction to increase and the reaction to oxidize. Nonetheless, the slow crystallization of the solution causes irregular and large crystalline structures with an interior high surface area. The ability to fully control synthesis conditions over a long period of time provides the advantage of developing reproducible protocols. Requirement of special equipment and the long duration of synthesis are the disadvantages of this method [7].

The non-solvothermal method, which is a very easy method for the synthesis of MOF, takes place at or below of the solvent boiling point at room temperature or elevated temperatures and at ambient pressure. This method does not require high temperature and pressure, hence, high energy efficiency and low cost. Certain well-known MOFs (MOF-5, ZIF-8, HKUST-1) have been synthesized in a short time at room temperature by mixing only the starting materials and subsequently precipitation. Increased reaction temperatures lead the change in the framework structure. The temperature increase may be necessary for the occurrence of effective reaction and crystallization rates [8].

Special equipment is not needed for non-solvothermal synthesis. In this method, the choice of salt for the metal source as well as the choice of solvent and the organic linker is important. It is possible to change the pH and temperature values for maximum efficiency of the targeted MOF. For the formation of a precipitate, the reagent concentrations should be selected so that the nucleation conditions are reached or the temperature should be increased. The concentration gradient can be generated by slow

cooling of the solution, solvent stratification or by slow diffusion of the one of the reagents [7].

2.1.4.2 Alternative Methods

Solvothermal and non-solvothermal methods generally require a heat-induced energy to perform the reaction. The synthesis of MOF generally occurs at a reaction temperature of 25 °C to 250 °C in a solvent. It is possible to use alternative methods where the temperature required for the reaction to take place, comes from another source. Microwave-assisted synthesis, mechanochemical synthesis, sonochemical synthesis and microfluidic synthesis can be examined under alternative synthesis. The different types of conditions can be used in each of these methods (such as pressure and reaction time) to obtain the different particle morphology [8].

The method of microwave synthesis is commonly utilized for the rapid synthesis of nanoporous materials under hydrothermal conditions. This technique has advantages such as narrow particle size distribution, phase selectivity and easy morphology control as well as rapid crystallization. Commercial microwave equipment has optical fiber temperature and pressure control devices and supplies adjustable power output. In microwave-assisted synthesis of MOFs, the substrate mixture in a suitable solvent is transferred to a Teflon tank and sealed and placed in the microwave unit. The heating is then carried out for a desired period at the appropriate temperature. The oscillating electric field applied in the microwave-assisted approach is connected with the permanent dipole moment of the molecules in the synthesis medium which induce molecular rotations. This causes the liquid phase to heat up rapidly. [13].

Since the microwave reaction directly interacts with the molecules in the system, the determination of solvent should be done carefully. The amount of microwave radiation exposed to the system is an important parameter and should be checked. This method has advantages such as rapid nucleation kinetics, short reaction time, crystal growth and high yield of products. On the other hand, there is almost no by-product produced in this method. Therefore, it does not require purification of synthesized particles. Even so, there are worries about the safety of this method. Another disadvantage is that the morphology of the particles and phase purity can vary greatly if the conditions of synthesis cannot be controlled well enough. The reproducibility of MOF particles is

significantly reduced [8]. Figure 2.3 shows microwave-assisted synthesis scheme of MOF.

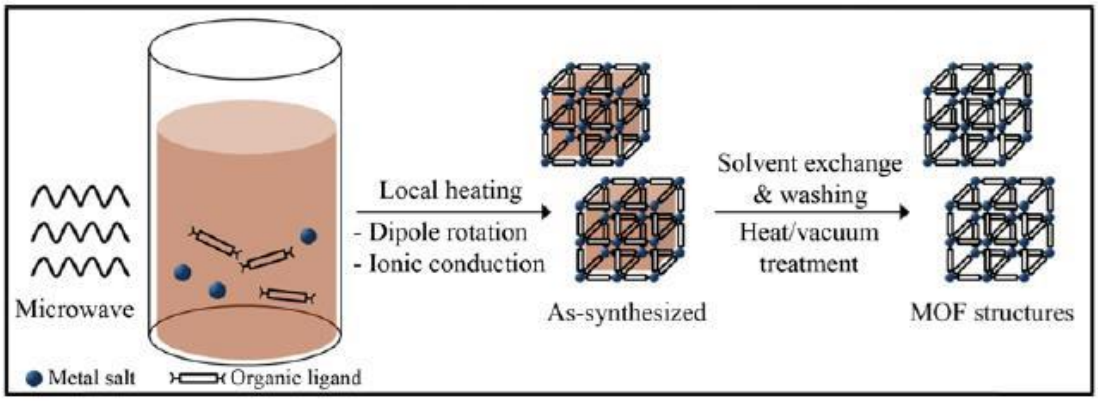


Figure 2. 3 Microwave-assisted MOF synthesis [13]

The sonochemistry phenomenon is a phenomenon in which molecules are subjected to chemical transformation by intensive ultrasonic radiation (20 kHz – 10 kHz). Ultrasonic inducations cause physical and chemical changes in a liquid due to the cavitation process, which allows the formation, growth and sudden collapse of bubbles. This phenomenon creates local and short-lived hot points with high temperature and pressure. The excessive conditions assist chemical reactions with the rapid formation of excess crystallization nuclei [13]. The diagram of sonochemical synthesis for MOFs can be seen in the Figure 2.4.

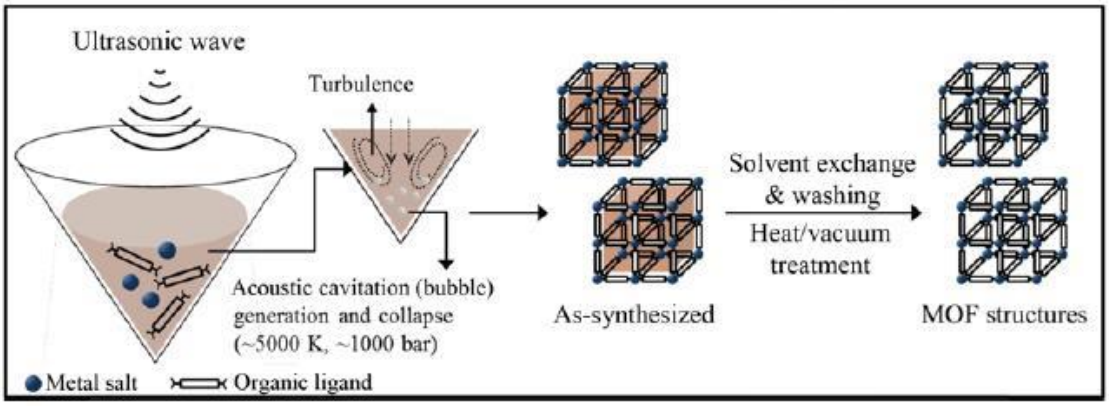


Figure 2. 4 Sonochemical synthesis of MOFs [13]

Sonochemical techniques provide a homogenous nucleation center and a significant reduction in crystallization time compared to traditional hydrothermal methods [11].

Electrochemical synthesis method is not well understood yet for the synthesis of MOF. The research groups focused on environmentally friendly, high energy efficiency, no traditional electric heating system and rapid MOF synthesis methods. Nevertheless, it is

well-known that MOFs should have nanosized crystals to be used in some applications and this method is used since the MOFs obtained by this method are generally in nanoscale [8].

In the electrochemical synthesis of MOFs, metal ions occur in consequence of an electrochemical process. The metal ions are obtained during the dissolution of the anode in the reaction mixture including dissolved linker molecules and an electrolyte (Figure 2.5). This enables to prevent the generation of anions during the reaction and to initiate the continuous processes required for large amounts of MOF synthesis [7].

The advantageous aspect of this method is the high product yield due to continuous processes. However, due to the low quality of the product, it is not a preferred method [8].

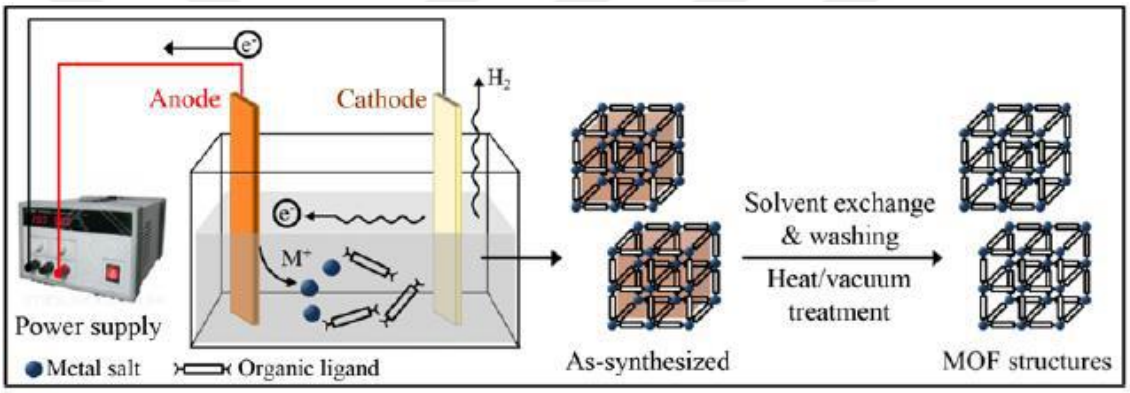


Figure 2. 5 Electrochemical MOF synthesis [13]

In the mechanochemical method, a chemical transformation occurs due to the mechanical breakage of interior molecular bonds. The mechanochemical reactions can also be performed at room temperature without using any solvent. Small MOF particles can generally be obtained with short reaction periods between 10 and 60 minutes. The preference for metal oxides as an initial material only produces water as a by-product compared to the preference of metal salts. [13].

The scheme of mechanochemical synthesis for MOFs is as shown in the Figure 2.6 [13].

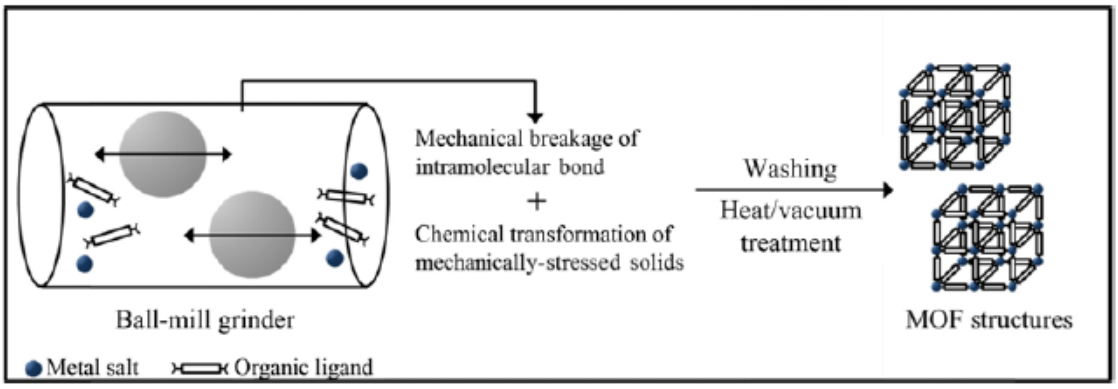


Figure 2. 6 Mechanochemical MOF synthesis [13]

One of the most attractive aspects of this solvent-free method is its suitability for large-scale environmental production. Avoidance of organic solvents and high temperatures makes this technique safer than conventional solvothermal techniques [8].

2.1.5 Applications of MOFs

Over the last few years, MOFs have been used frequently in gas adsorption, drug delivery, separation and catalysis applications. In other respects, due to their high surface area, pore volume, pore size adjustment and easy modification to metal nodes and ligands, MOFs are very suitable for enzyme immobilization applications. Furthermore, MOFs are perfectly suitable for stabilization of the enzyme construct into specific host-guest interactions or encapsulation. The number of studies involving enzyme-MOF composites is increasing day by day and new methods are being experienced. Still, specifically the subject of enzyme immobilization into/onto MOFs is considered less. Even though, the characteristics and applications of enzyme-MOF composites have been detailed, optimization of process and newly developed procedures for the preparation of enzyme-MOF composites have not been widely examined [9].

Studies focusing on MOFs and biomacromolecules have led to the discovery of bio-composites with promising properties in the storage and delivery of biopharmaceuticals and biosensing bio-catalysis fields. Biomimetric mineralization is one of the new methods for the synthesis of MOF bio-composites, giving positive results for bio-based applications [14].

2.1.6 Zeolitic Imidazolate Frameworks (ZIFs)

Zeolitic Imidazolate Frameworks which are new class of MOFs consist of tetrahedral metal ions (M=Zn or Co) bridged by Imidazolate (Im). Due to the fact that uniform pore structure and large internal surface area, this 3D structured framework can take place in catalysis, molecular separation, gas adsorption and storage. Depending on the similarity of their M-Im-M angle to the Si-O-Si angle (1458), they mostly preferred in zeolites. In a wide range of ZIFs with zeolite type tetrahedral topologies are synthesized as a new class of MOFs recently [15].

As regards to nomenclature of ZIFs, the number "n" of ZIF-n is entitled randomly by the first reporter authors. Although all ZIFs includes inorganic part of Zn or Co and imidazole-based derivative linkers and all these materials have nearly similar chemical structure, they have pretty different surface areas, morphology, pore diameters and crystal size which leads to multiple applications [12]. The topologies of some ZIFs and also their metal and inorganic linkers were shown in the Table 2.2.

Table 2. 2 The topologies of some ZIFs and also metal and inorganic linkers [12]

ZIF Framework	Topology	Metal	Linker
ZIF-8	Sodalite	Zn	5-methylimidazole
ZIF-90	Sodalite	Zn	Imidazolate-2-carboxyladehyde
ZIF-82	Gme	Zn	Chloronitroimidazole Nitroimidazole
ZIF-6	Gis	Zn	Imidazole
ZIF-21	Lta	Co	Purine
ZIF-67	Sodalite	Co	2-methylimidazole
ZIF-95	Poz	Zn	5-clorobenzimidazole

Topology of ZIFs strictly relies on the production parameters, which are solvent, reaction periods, metal source and imidazolate ligand functionalities. Imidazole is formed from two non-equivalent amine groups in five-membered ring. When the NH group of imidazole is deprotonated, a bidentate ligand is procured which is a requisite for generating supramolecular frameworks. This situation depends on the substitution in the position of 2, 4 or 5. For example, when additional group is get to the 2 position of imidazole linkers, the sodalite SOD topology appears while the RHO is obtained in the

4 and 5 position [12]. Figure 2.7 illustrates some of the ZIFs classified according to their topology.

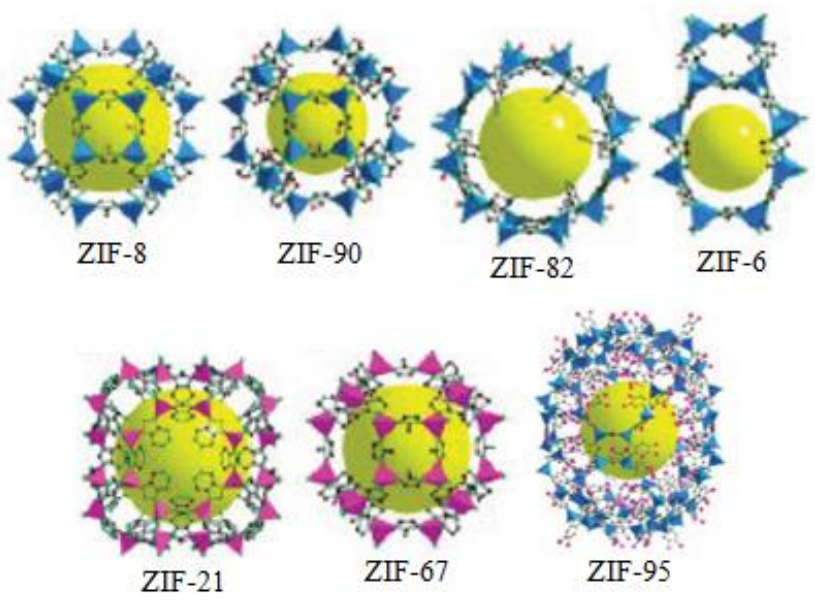


Figure 2. 7 Examples of ZIFs classified by topology [12]

2.1.6.1 ZIF-90 Synthesis

ZIF-90 is a well-known example of metal organic frameworks. In the previous ZIF-90 synthesis studies, organic solvents such as dimethyl formamide (DMF) or methanol were used. However, by the reason of its large size, DMF can easily adhere into the pores of ZIF-90 and reduce the accessible surface area. Besides organic solvents are costly and environmentally harm. Usage of water as an eco-friendly resolver has been considered in the synthesis of ZIF-90 [17].

Structure of ZIF-90 was shown in Figure 2.8. It can be seen that carbon, hydrogen, nitrogen, oxygen and zinc are observed in the structure of ZIF-90.

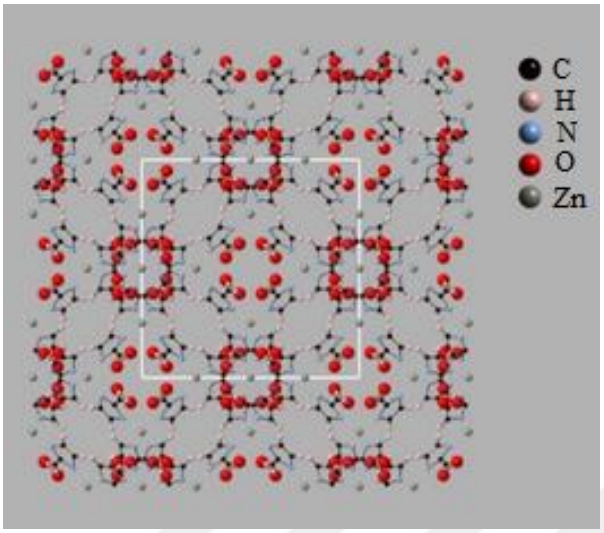


Figure 2. 8 Structure of ZIF-90

The following figure (Figure 2.9) illustrates the formation of ZIF-90. The reaction of the Zn^{+2} salt with the 2-imidazolatecarboxaldehyde organic ligand results in the ZIF-90.

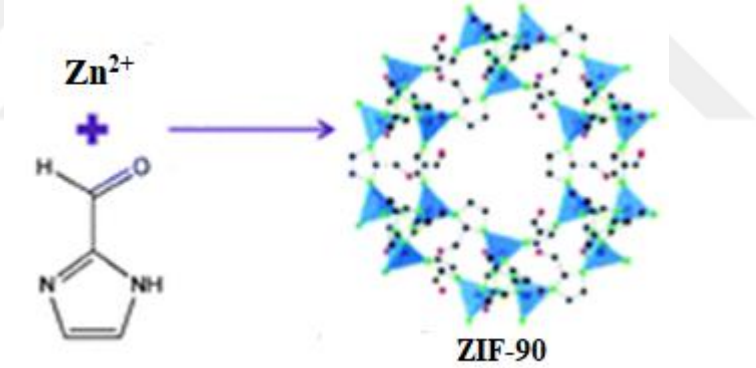


Figure 2. 9 Formation scheme of ZIF-90 [16]

2.1.6.2 ZIF-8 Synthesis

ZIF-8 is the most examined ZIF which is consisted of Zn tetrahedral clusters and 2-methylimidazolate linkers (Figure 2.11).

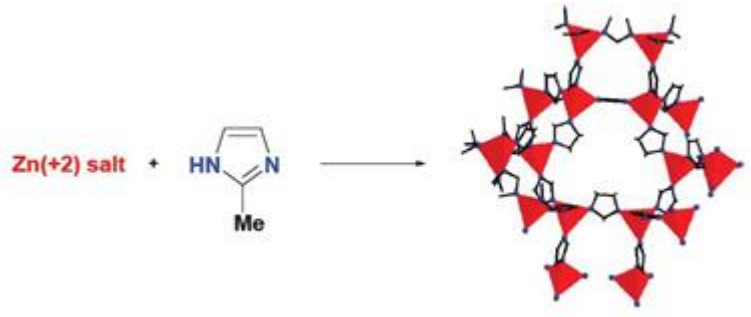


Figure 2. 10 Formation scheme of ZIF-8 [12]

Sodalite topology of ZIF-8, is shown in Figure 2.12. It can be seen that ZIF-8 consists of carbon, hydrogen, nitrogen and zinc. ZIF-8 network has large pores of 11.6 Â, with small apertures 3.4 Â, cubic symmetry and cell dimension of 16.32 Â. The ZIF-8 framework can be produced by standard solvothermal or non-solvothermal synthesis or by other alternative synthesis methods [12].

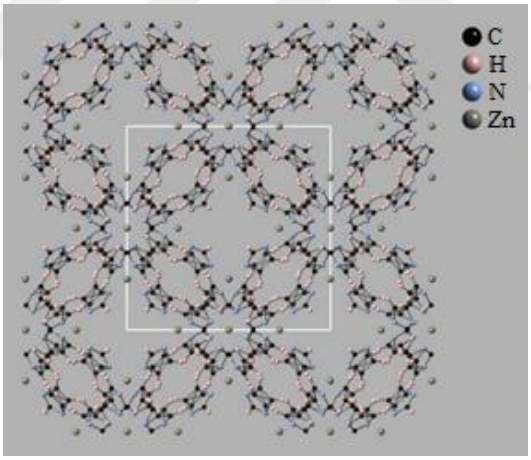


Figure 2. 11 Structure of ZIF-8

The shape and symmetry control of nanocrystals have been deeply researched in recent years because of the fact that the optical, optoelectronic, magnetic and catalytic properties of the synthesized material are affected by these parameters. It is reported that rhombic dodecahedron morphology of structure of ZIF-8 is the most sufficient one for several applications. Morphological formation of ZIF-8 is based on the synthesis conditions and the reaction period.

Evolution of the geometrical particle shapes over time determined for ZIF-8 can be seen in Figure 2.13 [12].

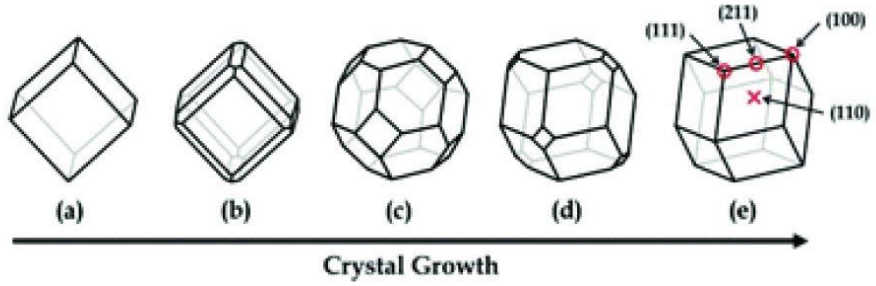


Figure 2. 12 Crystal growth evolution of ZIF-8 over time [12].

ZIF-8 was first represented by Yaghi et al. utilizing the solvothermal synthesis method in 2006. Unlike other MOFs formerly researched, ZIF-8 is insoluble and has outstanding chemical stability according to its ability to show resistance to hydrolysis, reflux organic solvents, water and aqueous alkaline solutions. This noticeable stability of ZIF-8 has been substantiated for two main reasons. Firstly, the bonding between the imidazolate N and the M(II) ion is competitive in strength with that solids includes covalent bonding. And the second reason is that ZIFs have hydrophobic pore which pushes away water molecules and prevent the MIm4 (M=Zn/Co). This feature of hydrophobicity of ZIF-8, which provides such extraordinary stability against tough chemical and thermal environments, is very useful for the ZIF-8 applications [8].

2.1.7 Characterization Techniques

Several characterization methods exist that are utilized in order to determine the different features of properties and structures of porous materials. Since small alterations in synthetic means can affect MOFs morphologies and properties and creates large changes. It is a necessity that complementary characterization techniques are managed to give information about MOFs particularly [8]. Some of the characterization techniques often used in this area are X-Ray Diffraction (XRD), Environmental Scanning Electron Microscope (ESEM), Brunauer-Emmet-Teller (BET) analysis and Fourier Transform Infrared Spectroscopy (FTIR).

The most remarkable of these characterization techniques is powder X-Ray Diffraction (XRD) that is an analytical technique and reveals understanding about the crystal structure of the materials that are researched at micro molecular level. The working mechanism of XRD is realized by exposing a crystalline material to a concentrated X-

Ray beam and monitoring the scattering intensity as a function of incident and scattered angle which enables the crystallographer to produce a 3D image of the material being scanned. Whether the compound has been synthesized before and fully characterized and able to compare to a prespecified crystalline material database, the compound can be identified by the initial measurement of the scattered X-Ray and intensities which provides an X-Ray diffraction pattern. For example, ZIF-8 has a known XRD pattern which has been done previously [8].

The known ZIF-8 XRD pattern can be used to compare the obtained XRD pattern of the product when synthesizing ZIF-8 applying a new procedure in a new experimentation. This can be seen in Figure 2.14, where a new acquired experimental XRD pattern is being compared to the known pattern of ZIF-8 [8].

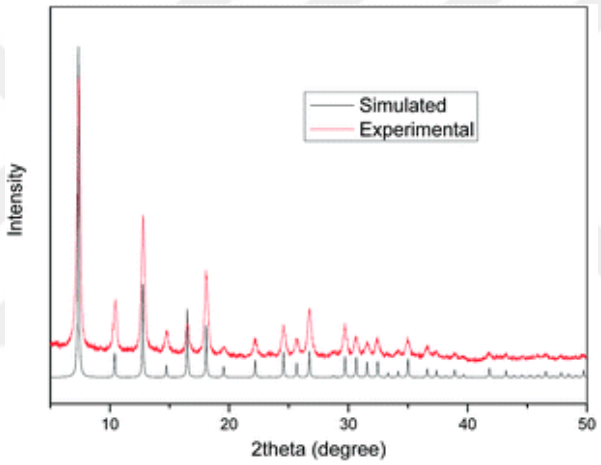


Figure 2. 13 Comparison of experimental result to simulated pattern from known ZIF-8 pattern [8]

Another important characterization technique is Electron Microscopy that directs electron beam at the material and provides an image enlarged many times. Electron microscope which gets an image much more effectively than a standard light microscope are generally used for nano-scaled or micro-scaled small porous materials like MOFs. In spite of its advantages and usefulness, the tough requirements of SEM, such as high vacuum conditions, complex preparation of the wet materials and biological samples (like living cells, proteins as antigens and enzymes), limits the application and wastes time of researchers. These problems can be overcome thanks to Environmental Scanning Electron Microscope (ESEM) that allows a gaseous environment, wet conditions and less conventional preparations [17].

Furthermore, Fourier Transform Infrared Spectroscopy (FTIR) is another method for structural characterization of crystalline materials and is used to indicate the chemical functional groups in a sample. Atoms of a molecule change their relative motion by vibrating which occurs through a way called as degree of freedom which can be electronic, rotational, translational and vibrational. When wide-spectrum infrared radiation is sent to covalent bonded molecules, some part of IR is absorbed by the molecule while some part of it is transmitted. Absorbed wavelengths represent the transitional energy between the levels of the degree of freedom of the corresponding molecule. In FTIR spectroscopy, the vibrational transitions are the most important ones and there must be a change in the dipole moment of the vibrating molecule for IR absorption to occur when the frequencies of the IR photon match with the vibrational energy of the molecule. The resulting IR spectrum is the molecular fingerprint in which represents the information about functional groups and characterize different molecules [18].

2.2 Enzymes

Mankind has examined the nature in order to find resolution some of the complicated problems such as aerodynamics, self-healing, catalysis and solar energy harvesting [1]. For certain, enzymes are one of the most significant biomacromolecules for life [2]. Enzymes consist of linear series of amino acids. Amino acids establish complex structures with highly specific catalytically active sites [1]. Enzymes are selective, influent and eco-friendly biocatalysts which catalyze life-sustaining biological transformations [2]. They can take places in numerous of large-scale processes such as the manufacturing of fine and pharmaceutical chemicals [1]. Enzymes can be utilized in biosciences and biotechnologies. They can be used in biofuel production, food processing, agricultural feeds, polymer synthesis and the paper industry [3]. Furthermore, by virtue of their easy production conditions, enzymes have been greatly admitted in varied fields [19]. On the other hand, such practical applications are prevented because of sensitive nature of enzymes, such as low thermal stabilities, limited optimum pH ranges, insufficient tolerances to most organic solvents and many metal ions, etc. Excessive amount of the enzyme is undesirable in synthetic processes as it limits the conditions required during enzyme denaturation. Additionally, enzymes can cause unwanted contamination in the desired product. Therefore, instead of using

homogeneous enzymes, operating heterogeneous immobilized enzymes is one of the significant methods for enhancing the performances of enzymes [2].

2.2.1 Enzyme Immobilization

Enzymes have high reaction specificity, low toxicity and high catalytic activity. Even so, the stability of aqueous solutions of free enzymes is a critical point that can hinder the use of enzymes in different applications. In addition, the loss of catalytic activity during the reaction of free enzymes are among the problems that can be experienced. It is possible to overcome such problems by means of enzyme immobilization [4]. Immobilization can be used for increasing stability and recoverability of enzymes and this method causes decreasing of cost [1]. Biological functions of the enzymes can be maintained with the usage of a convenient support under various reaction conditions [5]. Throughout biochemical reactions, to preserve enzymes' structural stability is highly challenging [19]. The use of organic solvents in immobilization processes may deactivate some regions of the enzyme or the active parts of the enzyme may be blocked. On the other hand, the enzyme mismatch between the external supports and the enzyme-substrate limits are also unfavorable conditions during enzyme immobilization [4]. Even though their expensiveness, immobilized enzymes are commonly used [19]. Many immobilized enzymes exhibit higher stability than free enzymes by reducing their mobility [4]. Due to their sophisticated functions, metal organic frameworks (MOFs) have been recently utilized to immobilize enzymes [5].

Metal organic frameworks have many promising properties that indicates interests for enzyme immobilization [1]. The mild operating conditions of surface attachment of MOFs make it idealize for prevention of structure and activity of enzymes [2]. Given the fact that MOFs are formed of both organic and inorganic components, it's possible that several interactions between MOF support and enzyme can be occurred such as hydrogen bonding, including salt-bridge formation; other van der Waals forces, including dispersion forces; and covalent or coordinative bonding. For larger and heavier macromolecules, dispersion forces exhibit stronger interactions, which scales with the number of polarizable electrons, whereas often negligible for small molecules. Size matching of MOF pores to enzyme axes ought to increase dispersion interactions due to the strength of these interactions immensely depends on the distance. Uniform loading, less leaching and an understanding of local environment around the

immobilized enzyme can be allowed by virtue of the crystalline and ordered nature of MOFs. Structure parameters of MOFs such as surface area along with pore size, shape and volume can be optimized for immobilization and encapsulation of specific enzymes due to the adjustable structures of MOFs. Finally, in order to well immobilization and prevention of enzymes to be utilized under the compelling catalytic conditions, MOFs can be designed to be enduring under rough thermal, mechanical and chemical conditions. In spite of the fact that immobilization of enzymes onto the MOFs' surface can be done, in the light of this information, researches about immobilizing enzymes inside MOFs (encapsulation) is centered on laying emphasis on catalytic applications. Encapsulation is the most explicit possible advantage way in order to inhibit the physical enzyme denaturation for example, to heating, dehydration, or changes in ionic strength of solution, while, with good size matching between enzymes and MOF pores, encapsulation can also utilize to hinder deactivation of enzyme by the way of aggregation with [1].

Alongside the potential utilities and advantages of enzyme immobilization, the selection of immobilization method and matrix is important and required to specify wisely to minimize the smallest loss of enzymatic activity because the chances in immobilization matrix and method affect and make changes in the physical and chemical properties of enzymes [2].

Immobilization of enzymes is promoted via bonding and non-bonding formation interactions between enzymes and solid supports. Generally, MOF-enzyme bio-composites can be investigated under five main methods in terms of their synthetic approaches; surface attachment, covalent bondage, pore encapsulation incorporation de Novo and co-precipitation [1]. While covalent bondage incorporate weak interactions like van der Waals interaction, π–π interaction or hydrogen bonding, the other three are the based on stonger forces.

2.2.1.1 Surface Attachment

Because of the poor interaction between enzyme and MOF surface, the binding of enzyme on the MOF's surface is one of the easiest proceedings. This procedure enables to pre-synthesize of MOFs and enables the synthetic conditions to reach the denaturation ranges of the target enzyme. Furthermore, because of the fact that nature of the interactions between MOF and enzyme is non-specific, a great various range of

MOFs could be applied as the immobilization matrix (there is no necessity for the existence of particular functional groups on the MOF or the pore size) [2]

Surface attachment procedure could be combined with a reticulation step of the protein by using cross-linking agents such as glutaraldehyde because of the potential protein leaching. As priorly notified for other supports, this method provides the advantage of immobilizing a large and precisely known amount of enzyme at the surface of a material. Hence, surface attachment is perfectly appropriate for classical electrodes such as glassy carbon and Pt, as well as for interdigitated microelectrodes [21].

2.2.1.2 Covalent Bondage

Bonding of enzymes on the MOFs' surface can be covalently formed and this linkage provides enhanced stability of recycling. Generally, Peptide bonds are formed by the free amino groups on the surface of enzyme or MOF and carboxylate groups on the surface of MOF or enzyme, respectively. This linkage is frequently rendered by carboxylate activating molecules such as N,N'-dicyclohexylcarbodiimide (DCC) or 1-ethyl-3-(3-dimethylaminopropyl) carbodiimide (EDC). Whereas the recyclability of the immobilized enzymes is expected to enhance significantly comparing to their non-covalently linked counterparts, in this manner, a large range of MOFs can be contained as immobilization support [2].

2.2.1.3 Pore Encapsulation

MOFs with mesoporous cavities submit a remarkable class of materials particularly for enzyme immobilization applications. Mesoporous MOFs have several fundamental advantages for enzyme immobilization: (1) very high enzyme loading thanks to increased pore volume and void space; (2) adsorption of enzymes into the cavities can be occurred physically that helps to improve stability and reduce leaching in recycled usage; (3) providing size selectivity for specific substrates due to the pore size of framework which is achieved hardly with surface enzyme immobilization. An additional protective layer, which prohibits aggregation through physical separation of enzyme moieties, is procured by physical adsorption of the enzyme into the pore cavity as enzyme altering species have to be able to diffuse through the pore channels to access the enzyme. Trivalent metal species can present chemical stability to MOFs in aqueous solutions and can be gathered up into clusters with high symmetry. For enzyme

immobilization, trivalent metal species are the predominant metal component of mesoporous MOFs [2].

Various studies have reported that the theoretic maximum enzyme encapsulation capacity has been approached despite relatively large crystals as compared with the size of enzymes. This situation states that the flexibility of enzymes should perform a notable role in the encapsulation process [2].

Encapsulated enzymes have been exposed minimal chemical modification, varying from traditional enzyme involved co-catalysis studies so that the activities could be maintained to the maximum extent [2].

2.2.1.4 Incorporation de Novo

The de Novo approach relates to the synthesis of organic and inorganic building blocks and the target enzyme together. This is useful to prevent formation of the framework and tertiary structures of the active enzyme. Channels or/and apertures, which are smaller than the size of the folded enzyme, have been presented by most MOFs. Therefore, MOF needs to be assembled around the enzyme. Underlying the novelty of this developing field, many few literature studies exist for this approach. But nevertheless, several groups of researches have reported that of its applicability of this pathway [1].

Generally, MOF selection is limited to large pore MOFs through; impregnation technique is used in order to load the large enzyme molecules into pre-synthesized MOFs in a specific preparation. However, de Novo approach enlarges the choice of MOF. As a matter of principle of de Novo approach, growth of the MOFs occurs around the enzyme molecules under a mild synthetic state. Due to this situation, pore sizes and structures do not have an important impact on MOF selection. MOF crystals could keep maintenance functionality of enzymes under a various reaction states with de Novo approach. The enzyme molecules are encapsulated in the tight mesoporous cavities left in the MOF crystals through growth of the framework around the enzyme molecules [5].

Figure 2.10 shows MOF formation around the enzyme molecule.

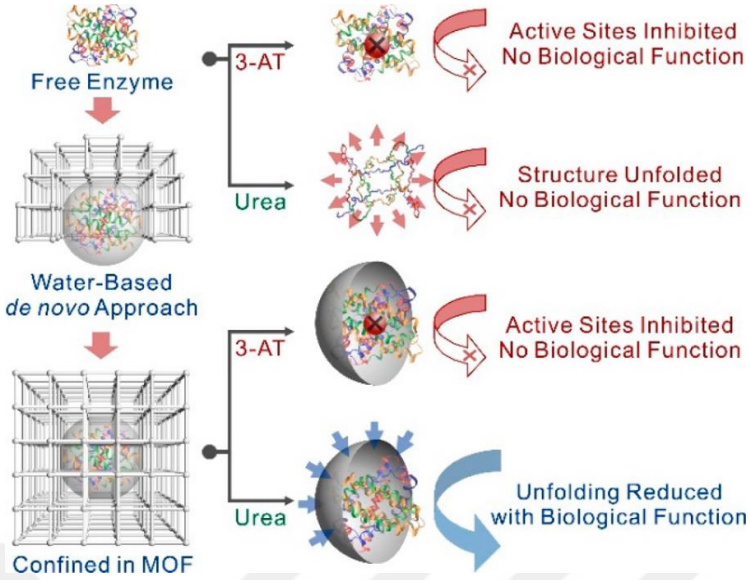


Figure 2. 104 De Novo approach and structural confinement [5]

2.2.1.5 Co-Precipitation

Enzymes can be immobilized in situ during the synthetic process by generating defects in the ZIF crystals as benefiting from that ZIFs in aqueous solutions have strongly mild synthetic conditions. According to the solution based synthetic methodology, guest molecule, whose size is larger than the pore openings, can be included into the MOF structure, where MOFs have a protective coating role. Preventing the leakage of guest molecules from the poles is one of the important advantages of ZIFs because of that ZIFs have the small pores. As well as that ZIFs act as a protective shell around immobilized enzyme, immobilized enzyme has remarkable operational stabilities at ultra-high temperatures, in a trypsin damaging environment or in pure organic solvents [2].

2.2.2 Horseradish Peroxidase Enzyme

Peroxidases are oxidoreductive enzymes obtained from animals, plants, fungi and microorganisms. They have charming bio-catalysis properties, broad substrate specificity, high stability and easy applicability. Under favour of these features, they have a wide range of industrial applications. They can oxidize various aromatic contaminants (peroxidases, dyes, phenols, aniline and heavy metal etc.). Peroxidase enzyme; catalyzes an electron oxidation of the aromatic substrate (AH2) in the presence

of peroxidase. This causes the formation of organic substrates (A2). Equation 2.7 shows the peroxidase catalyzed reaction [22].

$$AH2+H_2O_2 \rightarrow peroxidaseA+2H_2O \quad (2.7)$$

Peroxidases are divided into animal and plant peroxidase relying on their differences in structure and catalytic properties. They are widely used for the biological separation of industrial residues [22].

Plant peroxidases can be classified according to their main structure and origin as seen in the table (Table 2.3).

Table 2. 3 Classification of plant peroxidases [22]

Class	Member (EC number)	Origin	Industrial Applications
I	Cytochrome c peroxidase (EC 1.11.1.5)	Yeast, bacterium	Bioremediation
	Catalase-peroxidase (EC 1.11.1.6)	Bacterium, fungus	
	Ascorbate peroxidase (EC 1.11.1.11)	Plant	
II	Manganese peroxidase (EC 1.11.1.13)	Fungus	Pulp and paper manufacture
	Lignin Peroxidase (EC 1.11.1.14)	Fungus	Bioremediation
III	Peroxidase (EC 1.11.17, POX)	Plant	Biosensor Analytical and diagnostic kits Bioremediation

Class I consists of intracellular peroxidases, bacterial catalase peroxidases and ascorbate peroxidase. Class II includes extracellular fungal peroxidases such as secretory fungal peroxidases. Class III includes horseradish peroxidase (HRP), Soybean Peroxidase (SBP), turnip peroxidase (TP), bitter gourd peroxidase (BGP), potato pulp peroxidase, and secretory plant peroxidase such as ginger peroxidase [22].

The inadequacy of enzyme recovery and use is one of the negative factors limiting the application of peroxidases. Recently, immobilization studies have been performed for peroxidases. According to Longoria et al., enzymatic activity may be limited in the case

of binding of soluble enzymes to an insoluble support. However, it is thought that enzyme activity may be compensated by recent studies for peroxidases. Therefore, immobilization peroxidase is frequently used in wastewater treatment applications [22].

2.2.3 Enzyme Kinetics

Every biochemical reaction has its own specific enzymes. Due to lowering of the activation energy, enzymes serve in the similar way as do chemical catalysts. Because of the fact that fewer by-products are obtained and many enzymes confer high degrees of regioselectivity, high selectivity can be procured with enzyme biocatalysts [10].

Working with enzymes requires an understanding of enzyme kinetics. The basic enzyme kinetics can become clear by taking into the consideration of the equilibrium between the free enzyme (E), substrate (S), enzyme-substrate complex (ES) and products (P) in an enzymatic reaction as presented by Equation 2.8. The rate constants in this reaction k_1 and k_2 are attributed to the forward and reverse reactions, respectively [10].

$$E + S \overset{k_1\ k_{-1}}{\Longleftrightarrow} ES \overset{k_2}{\rightarrow} P + E \tag{2.8}$$

The enzyme, E, reacts with the substrate, S, to form the ES complex, then, , the product is formed after successive irreversible steps, and the enzyme can enter the new reaction cycle. Each steps of reversible reactions between enzyme and substrate can be seen in Equation 2.9 [23].

$$E + S \overset{k_1,\ k_{-1}}{\Longleftrightarrow} ES \overset{k_2,\ k_{-2}}{\Longleftrightarrow} E * S \overset{k_3,\ k_{-3}}{\Longleftrightarrow} E * P \overset{k_4,\ k_{-4}}{\Longleftrightarrow} EP \overset{k_5,\ k_{-5}}{\Longleftrightarrow} E+P \tag{2.9}$$

According to Equation 2.9, the enzyme and substrate form a loose ES association complex in a rapid equilibrium. Due to the interaction of the substrate with the catalytic center by rearranging the next step, a tight transition state complex E∗S is obtained. This step is carried to form the E∗P complex, which converts the substrate into the product. The E∗P transition state complex is transformed into the EP complex, which is a loose association complex before dissociation of the free product and the enzyme. This reaction sequence is symmetrical. Due to the product can also act as a substrate and the substrate as a product, this reaction can also be carried out in the reverse direction [23].

The rate of formation of the enzyme-substrate complex is described by $k_1[E][S]$ as well as the rate of destruction of the enzyme-substrate complex by $k_{-1}[ES]+k_2[ES]$. Through the rate of change of the enzyme-substrate complex is negligible, the relationship between the rates of the formation and the destruction of the enzyme-substrate complex can be equated as given Equation 2.10 where K_m is known as the Michaelis-Menten constant [10].

$$\frac{k_{-1}+k_2}{k_1} = \frac{[E][S]}{[ES]} = k = K_m \quad (2.10)$$

At the equilibrium point, the overall velocity of the enzymatic reaction is determined by the rate of the product formation which is the limiting step as well (Equation 2.11) [10].

$$v = k_2 [ES] \quad (2.11)$$

When the entire enzyme is formed to the enzyme-substrate complex, the maximum velocity for a given quantity of enzyme is reached. The maximum velocity is the velocity which relates to the total quantity of enzyme initially available (Equation 2.12) [10].

$$V_{max} = k_2 ([E]+[ES]) \quad (2.12)$$

In order to predict the reaction velocity, combining the Equations 2.10, 2.11 and 2.12 yields the well-known Michaelis-Menten equation which is presented in the terms of the Michaelis-Menten constant (Equation 2.13) [10].

$$v = \frac{V_{max}[S]}{K_m+[S]} \quad (2.13)$$

This equation describes a typical saturation curve where K_m equates to the substrate concentration when the velocity is half of the maximum velocity and shows the rate at which maximum velocity is reached which means high K_m means a slow rate and vice versa [10].

Kinetic constants in the Equation 2.13, V_{max} and K_m are required to be provided due to the prediction of the velocity of the enzymatic reaction. Conventionally, this is performed by the means of inversion of the Michaelis-Menten equation (Equation 2.14). V_{max} as the y-intercept and the reciprocal of K_m as x-intercept are obtained by plotting the reciprocal of substrate concentration (1/S) versus the reciprocal velocity (1/v) [10].

$$(1/V) = \frac{K_m}{V_{max}[S]} + (1/V_{max}) \quad (2.14)$$

In biochemistry, Equation 2.14 is actually known as the Lineweaver-Burk relationship and is used as the standard plotting for the calculation of the enzyme kinetic constants. However, it should be used only with extreme caution as it places the most reliance on the few points obtained at low substrate concentrations and, therefore, the points with the least accuracy. There are more reliable approaches can be used for obtaining the kinetic constants such as Eadic-Hofstee relationship or computer programs such as Matlab, Curve Expert etc. [10].

Matlab's Curve Fitting Program is used to obtain kinetic constants V_{max} and K_m and the graphical shown of those parameters. Matlab is also more preferable to provide the statistical results of the experimental data such as Regression Constant (R^2), confidential bounds and low and high values of kinetic constants [10].

There are two rate constants to characterize the Michaelis-Menten equation. First one is Michaelis constant K_m which specifies the affinity of substrate for enzyme (low K_m values mean high affinities), the second is Catalytic constant k_{cat} which indicates measure of the turnover rate of the enzyme [23]. Turnover number, k_{cat} which is the number of substrate molecules converted into product by an enzyme molecule in a unit time when the enzyme is fully saturated with substrate. Namely, k_{cat} constant gives information about how fast the reaction proceeds, number of catalytic cycles that each active site of the enzyme undergoes per unit time and so that the activity of the enzyme [20].

Turnover number, k_{cat}, which is in the units of s^{-1}, is presented at Equation 2.15 where E_T is total enzyme concentration:

$$k_{cat} = V_{max} / E_T \tag{2.15}$$

In order to determine the activity of the enzyme, the catalytic efficiency (or specificity constant) is supposed to be known which is obtained by the ratio of k_{cat}/K_m in the units of $M^{-1}s^{-1}$ (Equation 2.16). The catalytic efficiency indicates the best value to represent the overall ability of the enzyme to convert substrate to product [20].

$$k_{cat} / K_m = k_{cat}\, k_1 / (k_{-1} + k_2) \tag{2.16}$$

CHAPTER 3

EXPERIMENTAL STUDIES

3.1 Chemical Materials

All chemicals listed in Table 3.1 were used without additional purification and were obtained from Sigma-Aldrich. Milli-Q water was used for all aqueous solutions.

Table 3. 1 Materials list for ZIF and HRP encapsulated ZIF samples

	MW (g/mol)	**Storage [°C]**
Zinc nitrate hexahydrate ($Zn(NO_3)_2.6H_2O$)	297.49	15-25
Polyvinylpyrrolidone (PVP)	40	15-25
2-imidazolecarboxyaldehyde (ICA)	96.09	25
2-methylimidazole (HmIm)	82.10	15-25
Horseradish peroxidase (HRP)	44 (kDa)	2-8

In experiments, phosphate buffered saline (PBS), Potassium phosphate (KH_2PO_4), ABTS (2,2′-azino-di-(3-ethylbenzothiazoline sulfonic acid)), hydrogen peroxide (H_2O_2) were used and obtained from Sigma-Aldrich. BCA Reagent A (BCA Solution) and $CuSO_4$, which were used for BCA assay, obtained from G-Biosciences.

3.2 Devices

The laboratory equipment and characterization devices in below were used for synthesis and characterization of metal organic frameworks:

- Analytical Balance (Kern ABS-N/ABJ-NM)
- pH Meter (Hanna Instruments 387-4400)
- Magnetic Stirrer (SI Analytics™ 285416373)

- Ultrasonic Water Bath (VWR USC 300 TH Ultrasonic Cleaner)
- Centrifuge (Eppendorf Hermle ZK 380)
- Concentrator (Eppendorf 5301)
- Incubator (Heidolph Titramax 100 P/N: 544-11200-00)
- lyophilisator (Christ Alpha 1-4, B. Braun Biotech International)
- Multimode Microplate Reader (Tecan Spark)
- XRD (Bruker D8 Advance AXS)
- ESEM (Philips XL 30 FEG)
- FTIR (Bruker Optics Tensor 27 Spectrometer)
- EDX (EDAX Mahwah)

3.3 ZIF-90 Synthesis with Non-Solvothermal Technique

Non-solvothermal technique was used for the synthesis of ZIF-90 and samples were produced at room temperature. ICA, zinc nitrate hexahydrate and PVP were used as starting chemicals for the synthesis of ZIF-90 samples. The ZIF-90 synthesis steps were performed as shown below.

- Zinc nitrate hexahydrate was added into DI water.
- A solution of ICA and PVP was prepared in DI water. In order to obtain an homogeneous mixture, 500 mM PVP was added first and then, desired amount of ICA was added. This solution was kept in an ultrasonic water bath for 10 minutes.
- In a 25 mL beaker, the aqueous solution containing ICA and PVP was mixed.
- The zinc nitrate hexahydrate solution was rapidly poured into this mixture during mixing. This reaction was carried out at room temperature. The mixing time was 30 min and mixing rate was 500 rpm.
- After the reaction time completed, the solution was centrifuged at room temperature.
- After centrifugation, the precipitated solid was washed with PBS six times.
- Lyophilizator was used for drying of the obtained particles.

3.4 ZIF-8 Synthesis with Non-Solvothermal Technique

As in the synthesis of ZIF-90 samples, non-solvothermal technique was used for the synthesis of water-based ZIF-8 samples. 2-methylimidazole (HmIm) and zinc nitrate

hexahydrate was used as starting chemicals for the synthesis of ZIF-8. The water-based ZIF-8 synthesis steps were performed as shown below.

- Zinc nitrate hexahydrate was added into DI water.
- A solution of HmIm was prepared with DI water. In order to obtain a homogeneous mixture, this solution was kept in an ultrasonic water bath and degased for 10 minutes.
- In a 25 mL beaker, while the aqueous solution containing 2-methylimidazole was mix, the zinc nitrate hexahydrate solution was rapidly poured into this solution. This reaction was carried out at room temperature. In this method used in the synthesis of ZIF-8, the mixing time was 30 minutes and stirring rate was 500 rpm.
- After the reaction time completed, the solution was centrifuged at room temperature.
- After centrifugation, the precipitated solid was washed with PBS three to six times.
- Lyophilizator was used for drying of the obtained particles.

3.5 Enzyme Immobilization into ZIFs

Enzyme encapsulation in ZIF samples was carried out during the synthesis stage; HRP (Horseradish peroxidase) was added immediately after addition of zinc nitrate solution.

Synthesized ZIF and HRP immobilized ZIF samples with their codes were shown in Table 3.2. For instance, R90-2 was prepared with 500 mM PVP and 2:1 molar ratio of zinc/ICA; R8-025H10 was perapared with 1:4 molar ratio of zinc/HmIm and, 10 mg/mL HRP was immobilized to this sample.

Table 3.2 Codes for ZIF samples and HRP encapsulated ZIF samples

ZIF-90				ZIF-8		
Code	**Zinc/ ICA Molar Ratio**	**HRP (mg/mL)**	**PVP (mM)**	**Code**	**Zinc/ HmIm Molar Ratio**	**HRP (mg/mL)**
R90	2	-	50	**R8-2**	2	-
R90-2	2	-	500	**R8-025**	0.25	-
R90-2H1	2	1	500	**R8-025H1**	0.25	1
R90-025H1	0.25	1	500	**R8-025H10**	0.25	10
R90-2H10	2	10	500	**R8-05H10**	0.5	10
R90-1H10	1	10	500			

3.6 Chracterization of ZIFs and Enzyme Immobilized ZIFs

3.6.1 X-Ray Diffraction Analysis (XRD)

The samples were measured on a D8 Advance (Bruker AXS, Germany) with Cu Kα1,2 radiation. During the scan, running from 10 to 82 °2θ, with a step width of 0.019 °2θ and a total counting time per step of 134 seconds, the sample was rotated. The raw data was loaded into the Bruker Evaluation software DIFFRAC. EVA Version 5.0 for zero shift corrections and identifying the mineral phases presented.

3.6.2 ESEM and EDX Analysis

Scanning electron micrographs of the particles were obtained, using a Philips XL 30 FEG ESEM operated at an acceleration voltage of 12 kV at a chamber pressure of 133 Pa (1 Torr). To improve image quality, the specimens were sputtered with a thin conductive layer (5 nm Au/Pd 80/20) using a BAL-TEC MED020 coating system. For

energy dispersive X-ray (EDX) elemental analysis of the synthesized ZIF particles a liquid nitrogen cooled Sapphire Si(Li) detecting unit from EDAX (Mahwah, USA) was used. For spectra collection, the microscope was operated at 20 kV using a 100 μm aperture. The measurement time was 120 s.

3.6.3 FTIR Analysis

For the measurements, a Bruker Optics Tensor 27 spectrometer with room temperature deuterated tri glycinesulfate (RT-DTGS) detector and a Bruker Optics Platinum® ATR accessory (diamond crystal with one reflection) was applied (Bruker Optics, Ettlingen, Germany). All spectra were recorded at room temperature (22 °C) using the software Bruker OPUS 7.2. Spectra were recorded from 4000 cm^{-1} to 400 cm^{-1} with a resolution of 4 cm^{-1} against an air background. Sixty-four scans were co-added.

3.7 Determination of Enzyme Loading into ZIF samples

Enzyme loading into ZIFs was performed by measuring the amount of enzyme in the initial, final and washing solutions. Enzyme loading was calculated by the following equation. In this equation, E_f, E_i and E_w represent the enzyme concentrations (mg/mL) in the final, initial and washing solutions, respectively. V_i, V_f and V_w symbolize the volume of the initial, final and washing solutions (mL), while the mass (g) of the enzyme-ZIF composite, respectively.

$$L_{\text{enzyme-ZIF}} = \frac{(E_i V_i)-(E_f V_f)-E_w V_w}{m} \quad (3.1)$$

The encapsulation efficiencies were calculated by the equation given below.

$$\%\ \text{Encapsulation Efficiency} = 1 - \left(\frac{E_f+E_w}{E_i}\right)*100 \quad (3.2)$$

Reaction yields for prepared ZIF samples were calculated from the following equation.

$$\%\ \text{Yield} = \frac{m_{HRP-ZIF}}{m_{Zn(NO3)2}+m_{Organic\ Ligand}} *100 \quad (3.3)$$

In this equation, $m_{HRP\text{-}ZIF}$, $m_{Zn(NO3)2}$ and $m_{Organanic\ Ligand}$ represent the amount of prepared HRP-ZIF composite (mg), amount of $Zn(NO_3)_2$ in zinc nitrate hexahydrate and amount of organic ligand (mg), respectively.

3.7.1 Anaylsis of HRP

HRP enzyme concentrations were determined with Bicinchoninic Acid (BCA) Assay method by using the protocol supplied from G-Biosciences (1-800-628-7730, 1-314-991-6034) in Fluorescence Polarization Spectroscopy (FPS). Accordingly, 0.1 mg/mL, 0.3 mg/mL, 0.5 mg/mL, 0.7 mg/mL and 1 mg/mL concentration of standard HRP solutions were prepared with PBS solution in TECAN Spark Multimode Microplate Reader in order to prepare calibration curve. After addition of BCA reagent kit, color changes were observed in the prepared standard calibration solutions in 30 minutes incubation at 37 °C. Absorbance of the solutions was measured at 560 nm. The linear calibration formula, which gives the relationship between concentration and absorption values was found and the R^2 was calculated as 0.9941.

3.8 Determination of Kinetic Parameters

Kinetic parameters are one of the important parameters for enzymes. In order to determine the kinetic parameters of HRP enzymes in HRP-ZIF composites, ABTS and H_2O_2 were used as substrates (Eq. 3.4). Experimental details were described below.

$$H_2O_2 + \text{ABTS} \xrightarrow{\text{HRP/ZIF}} 2H_2O + \text{oxidized ABTS} \quad (3.4)$$

ABTS with different concentrations (0.2 mM, 0.5mM, 0.8 mM, 1.2 mM and 1.6 mM) in 50 mM KH_2PO_4, which pH value is 7, and H_2O_2 with 0.3% mass fraction were prepared. 90 µL ABTS in KH_2PO_4, 5 µL H_2O_2 with 0.3% mass fraction and 5 µL (1mg/mL) HRP-ZIF composites were added in a transparent microplate (Tecan, Nunc 96-well plate, F). Reaction kinetics were investigated at different substrate concentrations in order to determine oxidized ABTS (product) concentration. First, the microplate was incubated in the dark for 30 min and every 2 min absorbances were recorded at 415 nm for different ABTS concentrations. Then, obtained absorbance values at completion of the reaction were plotted against the initial ABTS concentrations. The slope of these plots were used to determine the product concentrations [P]. Initial product formation rate were obtained by the slope of [P]-t graphs. Absorbances of the prepared solutions were measured by using Fluorescence Polarization Spectroscopy (FPS) in TECAN Spark Multimode Microplate Reader. All kinetic experiments were performed triplicate at room temperature.

Michaelis-Menten equation constant, K_m, and maximum reaction rate, V_{max}, were calculated by plotting the reaction rate against the substrate concentration. These

parameters were obtained with the help of MATLAB 7.11.0 program. Then, k_{cat} was calculated by maximum reaction rate dividing to total enzyme concentration of HRP-ZIF composites. The ratio of k_{cat}/K_m corresponds to HRP efficiency for HRP-ZIF composites.

CHAPTER 4

RESULTS AND DISCUSSION

4.1 Energy Dispersive X-Ray (EDX) Results

ESEM image and corresponding EDX element mapping of prepared ZIF-90 sample (R90) was shown in Figure 4.1 and Table 4.1, respectively.

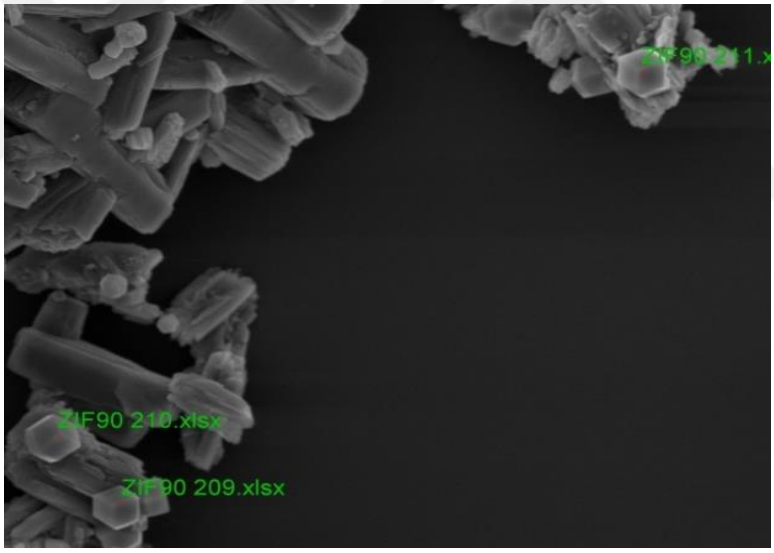


Figure 4. 1 ESEM image of R90

The regions marked with green colors (209, 210, 211) demonstrate the characteristic cubic structure (Figure 4.1). By means of EDX analysis, the elements contained in these regions and the percentages of these elements can be seen in Table 4.1. According to this table, EDX mapping of ZIF sample verified that Zn element exists in R90 particles. On the other hand, uniform dispersion of R90 particles did not observed. The percentage of zinc at the region labeled 211 is higher than compared to the region 209 and region 210.

Table 4. 1 Corresponding EDX element mapping of R90

Spectrum	C (%)	N (%)	O (%)	Zn (%)
R90-209	49.78	30.94	18.22	1.06
R90-210	50.28	30.03	18.21	1.48
R90-211	69.53	16.33	5.53	8.61
Mean	56.53	25.77	13.99	3.71

ESEM image and corresponding EDX element mapping of prepared ZIF-8 sample (R8-2) was shown in Figure 4.2 and Table 4.2, respectively. In this image, the regions marked with green colors (385, 386, 387, 388) demonstrate the characteristic rhombic structure of ZIF-8.

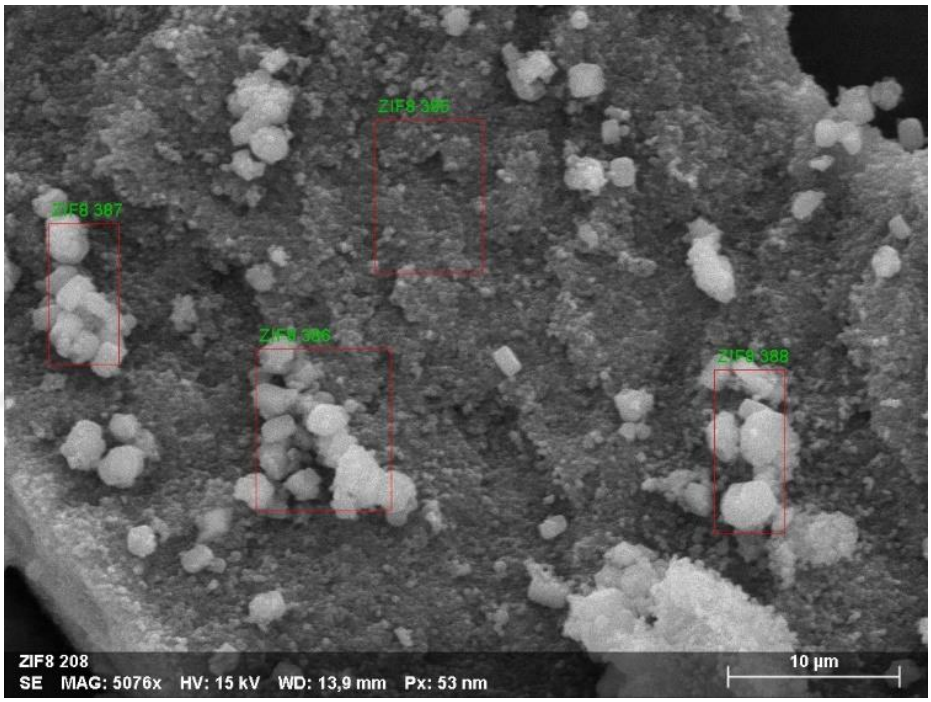


Figure 4. 2 ESEM image of R8-2

By means of EDX analysis, the elements contained in these regions and the percentages of these elements can be seen in Table 4.2. As seen from the table, there is no oxygen in contrast to the R90 sample. Carbon, nitrogen and zinc elements were detected in the marked regions of the R8-2 sample. It can be concluded that elements in R8-2 were dispersed within the structure uniformly.

Table 4. 2 Corresponding EDX element mapping of R8-2

Spectrum	C (%)	N (%)	Zn (%)
R8-2 385	65.31	27.90	6.79
R8-2 386	61.22	33.53	5.25
R8-2 387	66.59	28.24	5.17
R8-2 388	61.58	33.28	5.44
Mean	63.67	30.74	5.59

4.2 Effect of PVP Concentration

XRD patterns of prepared two ZIF-90 samples (R90 and R90-2) can be seen in Figure 4.3. Both samples have 2:1 molar concentration ratio of zinc nitrate hexahydrate and ICA. R90-2 contains higher amount of PVP with a 10-fold concentration than R90. R90 sample which was prepared with 50 mM PVP did not show a significant peak at 7.30 2θ angle. This peak, which is characteristic for the XRD pattern of the ZIF-90, was more clearly observed in the R90-2 sample, which was prepared with 500 mM PVP. Regarding XRD results, ZIF-90 synthesis can be improved by increasing PVP concentration.

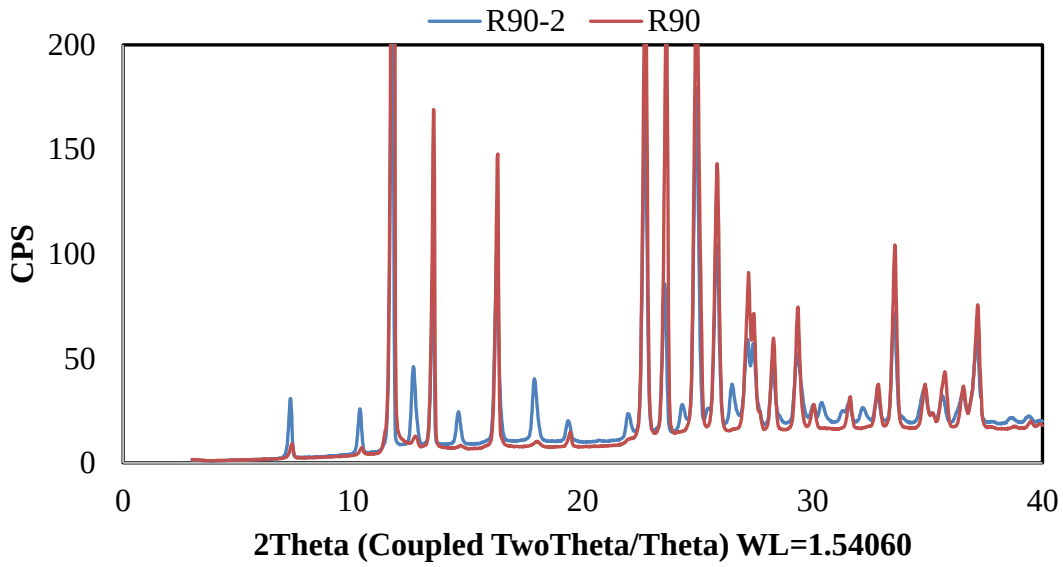
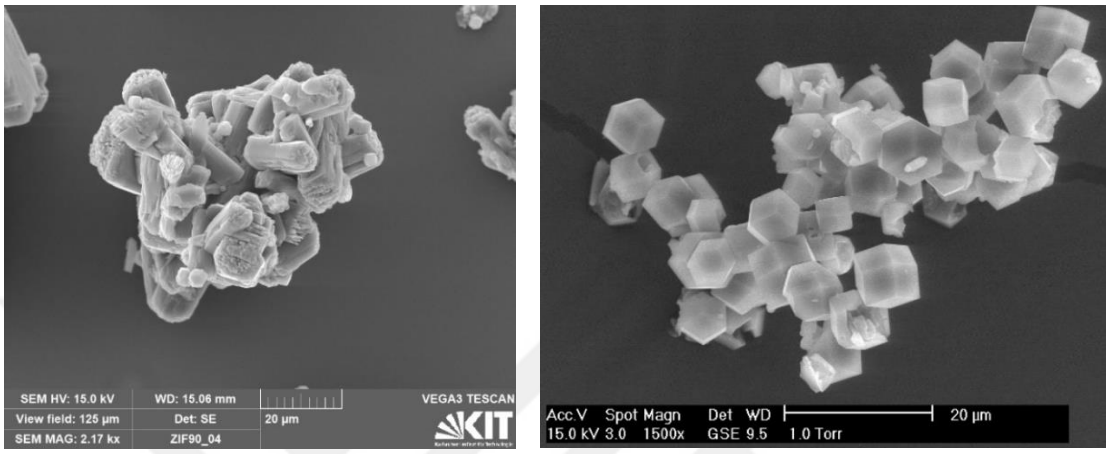


Figure 4. 3 XRD patterns of ZIF-90 samples at different PVP concentrations

PVP concentration can be arranged for the water based ZIF-90 systems in order to control the morphology of the crystals as a stabilizer [15].

Effect of PVP concentration were also investigated by using ESEM images of R90 and R90-2. As shown in Figure 4.4 (a) R90 sample exhibited non-uniform particles. Figure reveals that average 0.77 μm cubic shaped particles of R90.



(a) (b)

Figure 4. 4 ESEM images of (a) R90 and (b) R90-2

ESEM image of R90-2 sample was shown in the Figure 4.4 (b). Figure reveals that 1.91 μm average particle sizes of R90-2. The cubic shape of the R90-2 sample is more pronounced than the R90 sample and it can be seen that R90-2 sample appears to display the characteristic property of ZIF-90. From these figures (Figure 4.4 (a) and (b)), it can be seen how the concentration of PVP affects the ZIF particle structure. These results demonstrated that, the uniformity and crystallinity of water-based ZIF-90 system could be developed with higher PVP concentration.

It was observed that the significant positive results did not yield in case of PVP usage for the water-based ZIF-8 synthesis in contrast to the ZIF-90 synthesis.

4.3 Effect of Molar Ratios

4.3.1 Effect of Molar Ratios on Prepared ZIF-90 Samples

Molar ratio effects on ZIF samples were investigated. Figure 4.5 shows the XRD patterns of R90-025H1 and R90-2H1 samples. Although R90-025H1 sample with a molar ratio of 1:4 zinc/ICA did not show the characteristic peak of ZIF-90 at 7.30 2θ angle, R90-2H1 showed higher intensity peak at 7.30 2θ angle. It can be concluded that zinc/ICA molar ratio is very effective on the crystal structure of prepared ZIF-90 samples. Higher molar ratio should be used for ZIF-90 preparation.

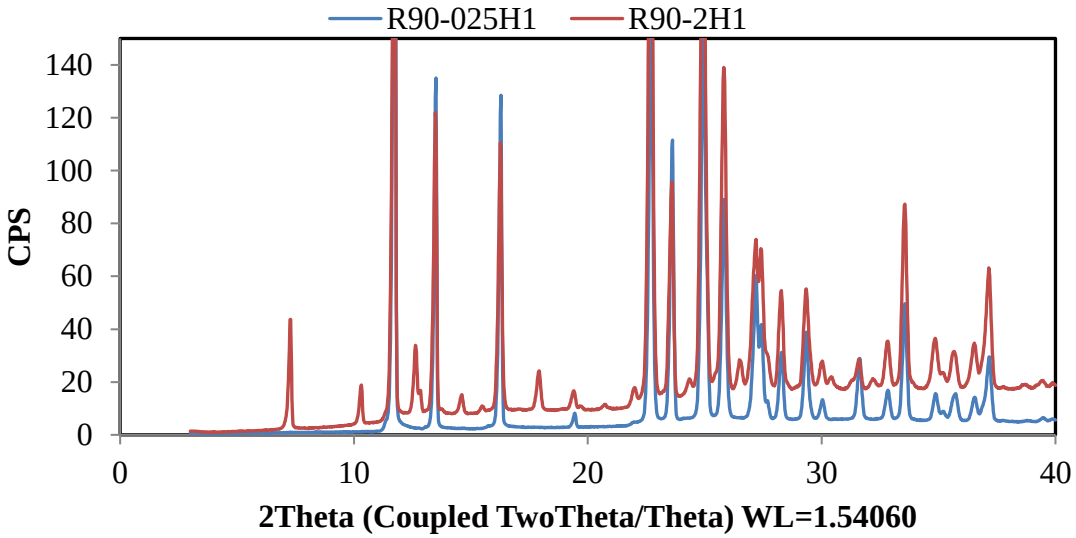


Figure 4.5 XRD Patterns of ZIF-90 samples at different molar ratios

4.3.2 Effect of Molar Ratios on Prepared ZIF-8 Samples

In Figure 4.6, it can be seen that XRD patterns of R8-025 and R8-2 samples, which have a molar ratio of 1:4 and 2:1 zinc/2-methylimidazole, respectively. All samples show prominent peaks at 7.09, 10.18, 12.51, 14.72, 16.49, 17.81 and 26.68 2θ angles. The XRD results of both samples overlaps with the ZIF-8 characteristic peak i.e. ZIF-8 formation occurred. It can be concluded that zinc/2-methylimidazole molar ratio is not effective on the crystal structure of prepared ZIF-8 samples.

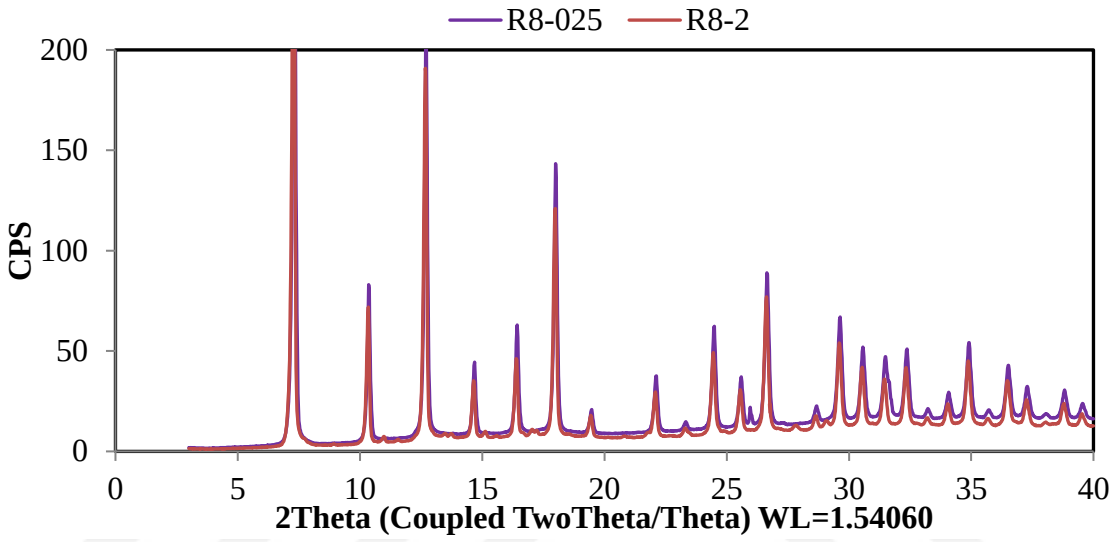
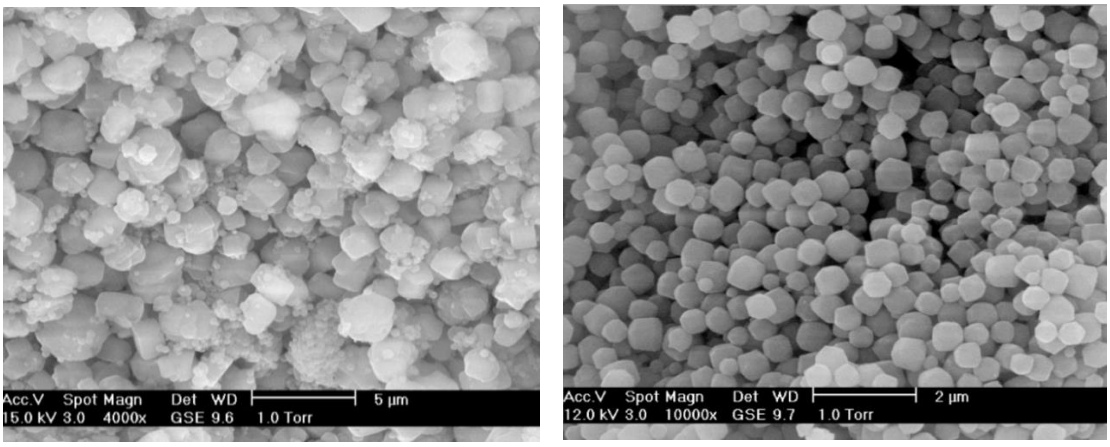


Figure 4. 6 XRD patterns of ZIF-8 samples at different molar ratios

Based on the ESEM results shown in Figure 4.7, we can see that the R8-025 sample which has average 101 nm sized particles exhibited smoother and typical ZIF-8 rhombic shaped particles. On the other hand, although R8-2 has average rhombic particles with 195 µm sized, it is non-uniform (Figure 4.7 (a)).



(a) (b)

Figure 4. 7 ESEM images of (a) R8-2 and (b) R8-025 samples

4.5 HRP Immobilization

The effects of HRP immobilization on ZIF-90 and ZIF-8 samples were investigated by using FTIR spectrum.

4.5.1 HRP Immobilization into ZIF-90 Samples

FTIR spectrum of prepared ZIF-90 (R90-2), HRP immobilized ZIF-90 samples (R90-2H1 and R90-2H10), and HRP enzyme was displayed in Figure 4.8. All HRP immobilized samples have the similar FTIR spectrum compared to R90-2. The R90-2, R90-2H1 and R90-2H10 samples have peaks originating from the Zn-O stretching modes at 569, 633 and 745 cm^{-1} [26]. The strong and broad peak seen at 2621 cm^{-1} indicates the O-H binding in all ZIF structures. Weak and broad peaks at 2849 and 2983 cm^{-1} can be shown as evidence for alcohol-induced O-H stretching bonds [29]. The peak seen at 1678 cm^{-1} is associated with C=O bonds in the structure of all synthesized ZIF-90 samples [27]. It can not be seen the characteristic FTIR peaks of HRP on the HRP immobilized samples. Hence, it can be concluded that none of HRP was immobilized onto the surface of ZIF-90 samples, in other words, all immobilized HRP was encapsulated into prepared ZIF-90 structure.

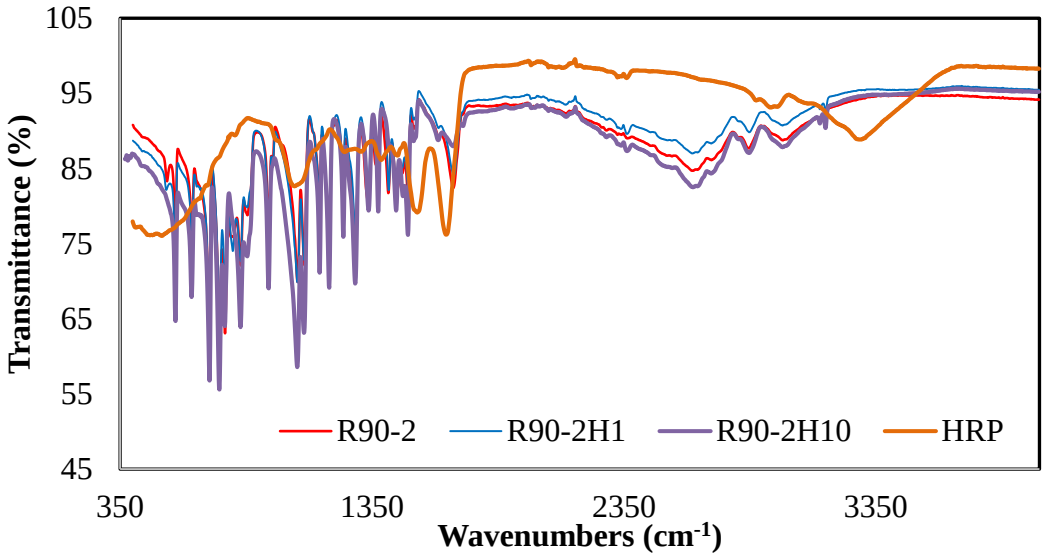


Figure 4.8 FTIR spectrum of HRP immobilized ZIF-90 samples

Figure 4.9 shows the XRD patterns of the prepared ZIF-90 (R90-2) and HRP immobilized ZIF-90 sample (R90-2H1). It was observed that the samples displayed very similar peaks at the 2θ diffraction angles (7.34, 10.35, 11.73, 13.36, 16.33, 22.86, 25.11). Considering this result, it was observed that the ZIF-90 crystal structure was preserved after immobilization with HRP enzyme.

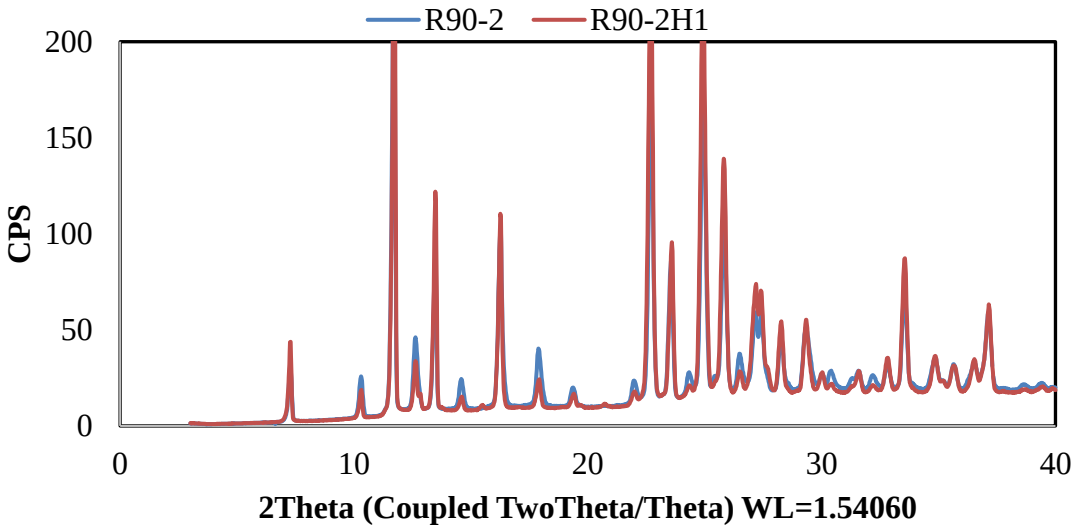


Figure 4.9 XRD patterns of HRP immobilized ZIF-90 samples

4.5.2 HRP Immobilization into ZIF-8 Samples

The FTIR spectrum of prepared ZIF-8 (R8-025) and HRP immobilized ZIF-8 samples (R8-025H1 and R8-025H10), and HRP enzyme were shown in Figure 4.10.

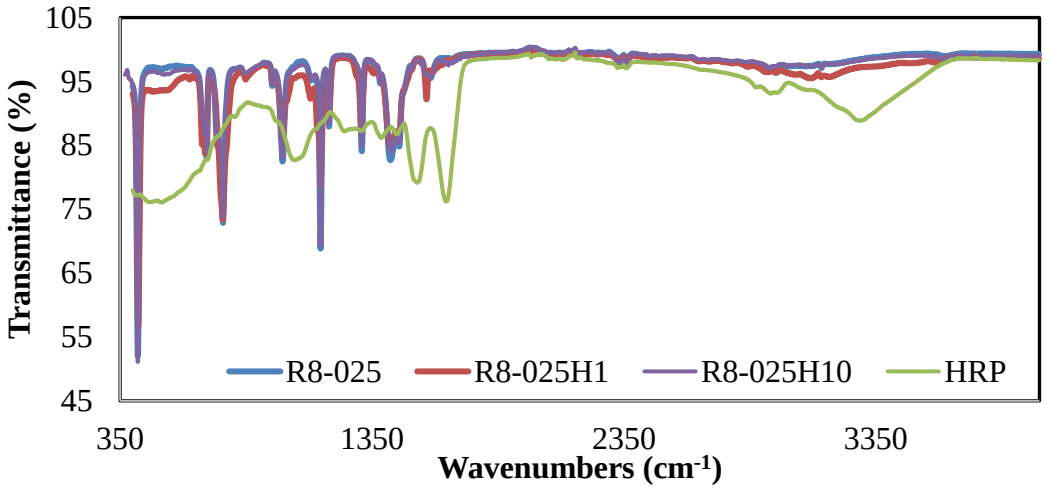


Figure 4. 10 FTIR spectrum of HRP immobilized ZIF-8 samples

All HRP immobilized samples have the similar FTIR spectrum compared to R8-025. ZIF-8 characteristic band from Zn-N stretching was observed at 421 cm^{-1} for all synthesized ZIF samples. In addition, peaks belonging to 900 -1400 cm^{-1} C-N bonds were observed (1027, 1145 and 1309 cm^{-1}). At 3118 cm^{-1}, the peaks showing that alcohol-induced O-H stretching were observed [30]. In addition, there is no characteristic FTIR peaks of HRP on the HRP immobilized samples. Hence, it can be concluded that none of HRP was immobilized onto the surface of ZIF-8 samples, in other words, all immobilized HRP was successfully encapsulated into prepared ZIF-8 structure.

Figure 4.11 shows XRD patterns of prepared ZIF-8 (R8-025) and HRP immobilized ZIF-8 sample (R8-025H1). It was observed that the samples displayed very similar peaks at the 2θ diffraction angles (7.48, 10.49, 13.11, 14.95, 16.62, 18.31, 26.95).

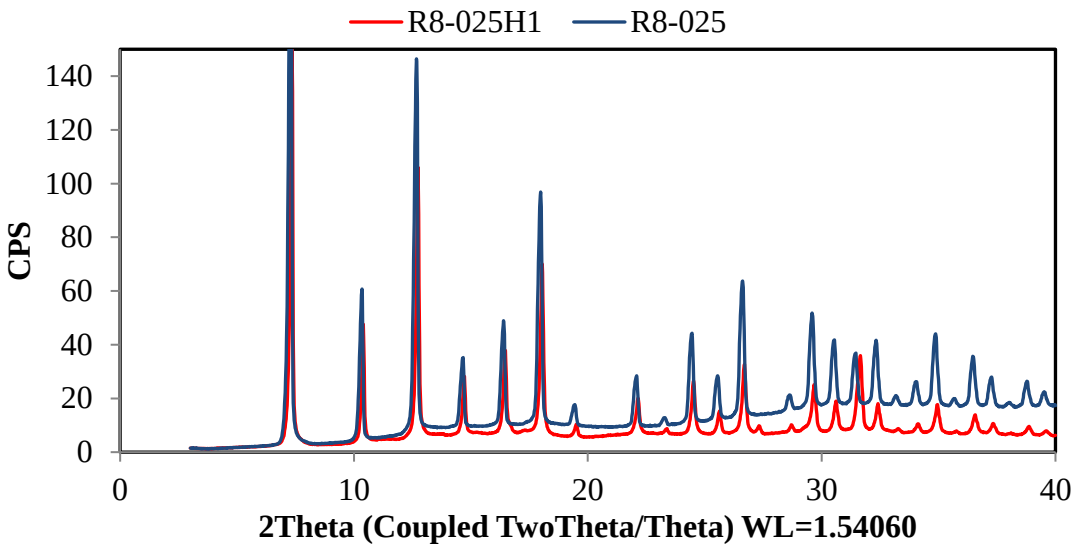


Figure 4. 11 XRD patterns of HRP immobilized ZIF-8 samples

All immobilized ZIF-8 samples correspond very well with the characteristic XRD pattern of ZIF-8. Based on this result, it can be said that the desirable ZIF-8 crystal structure was also preserved after immobilization of the HRP enzyme.

4.5.3 HRP Loading into ZIF Samples

In Table 4.3, encapsulation efficiencies, HRP loading and the yield of HRP-ZIF composites can be seen. As can be seen from Table 4.3, encapsulation efficiency, HRP loading and yield are significantly high for R90-1H10 sample, which was prepared with the high amount of organic ligand compared to R90-2H10. On the other hand, encapsulation efficiency, HRP loading and yield are high for R8-05H10 sample, which was prepared with the low amount of organic ligand compared to R8-025H10.

Table 4. 3 Encapsulation efficiencies, HRP loading and yield of HRP-ZIF composites

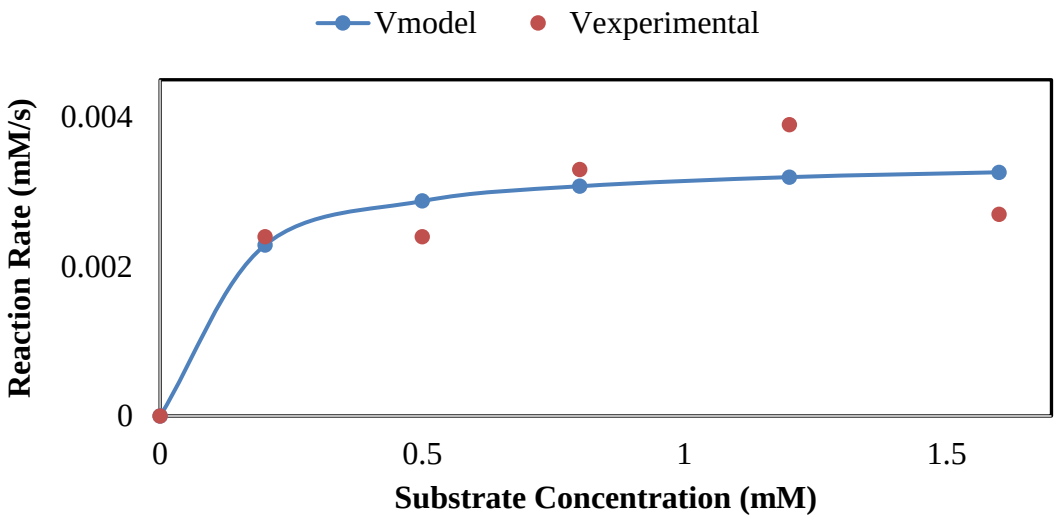
	R90-2H10	**R90-1H10**	**R8-025H10**	**R8-05H10**
HRP-ZIF (mg)	100.2	319.1	105.9	121.8
Encapsulation Efficiency (%)	5.79	39.31	17.65	39.13
HRP Loading (mg HRP/g HRP-ZIF)	11.55	24.64	33.34	64.26
Yield (%)	26.50	84.40	4.84	10.47

If we compare the best samples of each ZIF samples, although HRP loading of R8-05H10 is higher than R90-2H10, it can be concluded that prepared ZIF-90 sample showed the best results in the point of engineering approach due to the the yield of prepared ZIF-90 is significantly high (84.40 %).

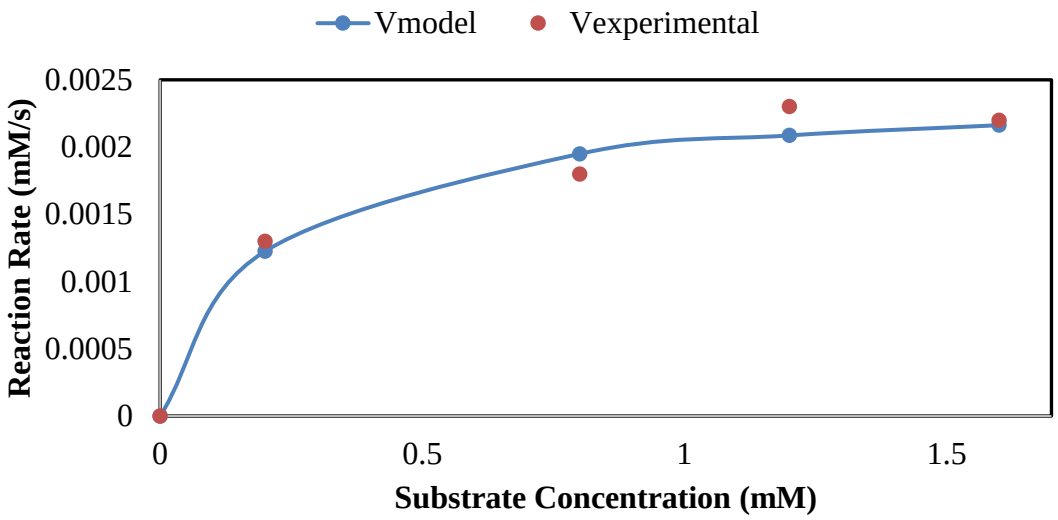
4.6 Enzyme Kinetics Results

ABTS oxidation reaction kinetics were investigated at different substrate concentrations in order to determine oxidized ABTS (product) concentration in the presence of HRP-ZIF composites. Obtained absorbances against time plot at different ABTS concentrations for each HRP-ZIF composites were given in Appendix B. The mean values of the absorbances at completion of the reaction were determined for each HRP-ZIF composites from Figure B.1-2. It was assumed that mean absorbance values at the equilibrium of the reaction correspond the product concentration. Data obtained from each mean absorbance values for different initial substrate concentrations were plotted, then, product concentrations were obtained by using the slope of these curves (Appendix C). The slope of the linear lines of the product concentration (until the plateau) versus time (Appendix D) gave the reaction rate. By plotting the reaction rate against the substrate concentration, K_m (Michealis-Menten equation constant) and V_{max} (maximum reaction rate) parameters were calculated according to the Michealis-Menten

equation (Eq. 2.13). Obtained Michealis-Menten graphs for R90-2H10 and R8-025H10 composites can be seen in Figure 4.12.



(a) R90-2H10



(b) R8-025H10

Figure 4.12 Michealis-Menten plots for (a) R90-2H10 and (b) R8-025H10 HRP-ZIF samples

The K_m and V_{max} parameters obtained from MATLAB 7.11.0 for each HRP-ZIF composite and the R^2 of the Michealis-Menten graphs were shown in Table 4.4. In addition, enzyme turnover rates, k_{cat}, were calculated by dividing V_{max} (mM/s) into the enzyme concentration (mM) in HRP-ZIF composites. The enzyme efficiency (k_{cat}/K_m)

of the HRP enzyme was calculated for each HRP-ZIF composite by dividing the k_{cat} value into the K_m constant (Table 4.4).

Table 4. 4 Michealis-Menten kinetic parameters, k_{cat} and enzyme efficiency values with the literature data

	K_m	**V_{max} (mM/s)**	**R^2**	**$E(10^{-5}mM)$**	**k_{cat} (s^{-1})**	**k_{cat}/K_m**
R90-2H10	0.1037	0.003473	0.8763	1.31	265	2552
R8-025H10	0.1965	0.002484	0.9808	3.79	66	334
Free HRP [31]	1.8	-	-	-	753	418
PCN333(Al) [31]	0.84	-	-	-	257	306

As can be seen from Table 4.4, although enzyme concentration in the reaction solution was higher in case of R8-025H10 sample, higher reaction rate was obtained with the prepared R90-2H10 sample. Moreover, enzyme efficiency of prepared ZIF-90 sample was significantly higher than prepared ZIF-8 sample. Feng et al. (2015) reported ABTS oxidation reaction kinetic results with the free HRP and HRP immobilized MOF structure [31]. Compared to our results, we hereby reported that prepared ZIF-90 samples in our study showed better enzyme efficiency than the literature and free HRP enzyme.

CHAPTER 5

CONCLUSION

In this study, the synthesis of ZIF-90, ZIF-8 and enzyme-ZIF composites were investigated. Characterization of these synthesized samples was done by various methods. The amount of enzyme at enzyme-ZIF composites were detected and kinetic parameters were determined. The results obtained from the experiments and investigations are given below.

- ZIF-90 and ZIF-8 samples were synthesized by non-solvothermal technique at room temperature. Enzyme immobilization was performed during ZIF synthesis. Particularly since ZIF-8 formation is known to be very fast, the enzyme was added immediately after the addition of zinc source to the organic ligand.
- The EDX characterization showed that prepared ZIF-90 samples contained C, N, O and Zn elements, while the ZIF-8 samples contained C, N and Zn elements as expected.
- ESEM images demonstrated that, the uniformity and crystallinity of water-based ZIF-90 system could be developed with higher PVP concentration. On the other hand, it was observed that the significant positive results did not yield in case of PVP usage for the water-based ZIF-8 synthesis in contrast to the ZIF-90 synthesis.
- Zinc/ICA molar ratio was very effective on the crystal structure of prepared ZIF-90 samples. Higher molar ratio should be used for ZIF-90 preparation. On the other hand, zinc/2-methylimidazole molar ratio was not effective on the crystal structure of prepared ZIF-8 samples. In addition, lower molar ratio resulted in lower particle size.

- FTIR spectrum of prepared ZIF-90 samples were displayed characteristics Zn-O stretching modes, alcohol-induced O-H stretching bonds and C=O bonds. FTIR spectrum of prepared ZIF-8 samples were displayed Zn-N stretching bonds, C-N bonds and alcohol-induced O-H stretching as expected.
- FTIR peaks of HRP immobilized samples showed that all immobilized HRP was encapsulated into prepared ZIF-90 and ZIF-8 structures.
- All HRP enzyme immobilized ZIF-90 and ZIF-8 samples corresponded very well with the characteristic XRD pattern of ZIFs. Then, it was concluded that ZIF-90 and ZIF-8 crystal structures were preserved after immobilization of the HRP enzyme.
- Both encapsulation efficiency, HRP loading and yield values were obtained significantly high for the prepared ZIF-90, which was prepared with the high amount of organic ligand. Contrastly, encapsulation efficiency, HRP loading and yield values were obtained low for prepared ZIF-8 samples, which was prepared low amount of organic ligand.
- Compared to both ZIF-90 and ZIF-8 samples, prepared ZIF-90 sample showed the best results in the point of engineering approach due to the the yield of prepared HRP-ZIF-90 is significantly high (84.40 %).
- In order to determine the kinetic parameters of HRP enzyme in HRP-ZIF composites, ABTS and H_2O_2 were used as substrates.
- Higher reaction rate was obtained with the prepared ZIF-90 sample. Moreover, enzyme efficiency of prepared ZIF-90 sample was significantly higher than prepared ZIF-8 sample. Prepared ZIF-90 samples in our study showed better enzyme efficiency than the literature and free HRP enzyme.

As a conclusion, ZIF-90 and ZIF-8 metal organic framework structures prepared successfully by using non-solvothermal method at room temperature. HRP-ZIF composite nanoparticles can be used effectively in ABTS oxidation reaction.

REFERENCES

[1] Majewski, M. B., Howarth, A. J., Li, P., Wasielewski, M. R., Hupp, J. T. and Farha, O. K., (2017). "Enzyme encapsulation in metal-organic frameworks for applications in catalysis", Royal Society of Chemistry, 19(29):4082-4091.

[2] Lian, X., Fang, Y., Joseph, E., Wang, Q., Li, J., Banerjee, S., Lollar, C., Wang, X. and Zhou, H., (2017). "Enzyme-MOF (metal organic framework) composites", Royal Society of Chemistry, 46:3386-3401.

[3] Kim, D. and Herr, A. E., (2013). "Protein immobilization techniques for microfluid assays", American Institute of Physics, Biomacrofluidics, 7(4):041501.

[4] Ocsoy, I., Dogru, E. and Usta, S., (2015). "A new generation of flowerlike horseradish peroxides as a nanobiocatalyst for superior enzymatic activity", Enzyme and Microbial Technology, 75–76:25-29.

[5] Liao, F.-S., Lo, W.-S., Hsu, Y.-S., Wu, C.-C., Wang, S.-C., Shieh, F.-K., Morabito, J. V., Chou, L.-Y., Wu, K. C.-W. and Tsung, C.-K., (2017). "Shielding against Unfolding by Embedding Enzymes in Metal-Organic Framework via a de Novo Approach", Journal of the American Chemical Society, 139:6530-6535.

[6] Huo, J., Aguilera-Sigalat, J., El-Hankari, S. and Bradshaw, D., (2014). "Magnetic MOF microreactors for recyclable size-selective biocatalysis", Royal Society of Chemistry, 6:1938-1943.

[7] Butova, V. V., Soldatov, M. A., Guda, A. A., Lomachenko, K. A. and Lamberti, C., (2016). "Metal-organic frameworks: structure, properties, methods of synthesis and characterization", Russian Academy of Sciences and Turpion Ltd, 85(3):280-307.

[8] Milburn, K., (2014). Synthesis and Characterization of ZIF-8 and ZIF-8/polymer composites, University of Liverpool, MSc Thesis.

[9] Cui, J., Ren, S., Sun, B. and Jia, S., (2018). "Optimization protocols and improved strategies for metal-organic frameworks for immobilizing enzymes: Current development and future challenges", Coordination Chemistry Reviews, 370:22-41.

[10] Clarke, K. G, (2013). Bioprocess engineering an introductory engineering and life science approach, Woodhead Publishing, Cambridge, UK.

[11] Dey, C., Kundu, T., Biswal, B. P., Mallick, A. and Banerjee, R., (2013). "Crystalline metal-organic frameworks (MOFs): synthesis, structure and

function", Acta Crystallographica Section B Structural Science, Crystal Engineering and Materials, B70:3-10.

[12] Schejn, A. M., (2018). Synthesis and catalytic activity of ZIF-8 and doped-ZIF-8 crystals: stability and cytotoxicity evaluation, PhD Thesis, Université de Lorraine.

[13] Lee, J. M. and Yeong, W. Y., (2016). "Design and Printing Strategies in 3D Bioprinting of Cell-Hydrogels: A Review", Advanced Healthcare Materials, 5:2856–2865.

[14] Doonan, C, Riccò, R., Liang, K., Bradshaw, D. and Falcaro, P., (2017). "Metal-Organic Frameworks at the Biointerface: Synthetic Strategies and Applications", American Chemical Society, 50:1423-1432.

[15] Shieh, F.-K., Wang, S.-C., Leo, S.-Y. and Wu, K. C.-W., (2013). "Water-Based Synthesis of Zeolitic Imidazolate Framework-90 (ZIF-90) with a Controllable Particle Size", Chemistry a European Journal, 19:11139-11142.

[16] Yang, T., and Chung, T. S., (2013). "Room-temperature synthesis of ZIF-90 nanocrystals and the derived nano-composite membranes for hydrogen separation", Journal of Materials Chemistry A, 1(19):6081-6090.

[17] Mouret, M., Bascoul, A. and Escadeillas, G., (1999). "Microstructural features of concrete in relation to initial temperature—SEM and ESEM characterization", Cement and Concrete Research, 29(3):369-375.

[18] Robinson, J.W., Skelly-Frame, E.M. and Frame, G.M., (2005). Undergraduate Instrumental Analysis, 6th Edition, Marcel Dekker, New York.

[19] Datta, S., Christena, L. R. and Rajaram, Y. R. S., (2013). "Enzyme immobilization: an overview on techniques and support materials", Biotech, 3:1-9.

[20] Berg, J. M., Tymoczko, J. L. and Stryer, L., (2002). Biochemistry, 5th Edition, W. H. Freeman and Company, New York.

[21] Gkaniatsou, E., Sicard, C., Ricoux, R., Mahy, J.-P., Steunou, N. and Serre, C., (2017). "Metal–organic frameworks: a novel host platform for enzymatic catalysis and detection", Royal Society of Chemistry, 4:55-63.

[22] Jun, L. Y, Yon, L. S., Mubarak, N. M., Bing, C. H., Pan, S., Danquah, M. K., Abdullah, E. C. and Khalid, M, (2019). "An overview of immobilized enzyme technologies for dye and phenolic removal from wastewater", Journal of Environmental Chemical Engineering, 7:102961.

[23] Bisswanger, H., (2017). Enzyme Kinetics Principles and Methods, Wiley-VCH, Third Edition, Weinheim, Germany.

[24] Mattos, C. and Ringe, D., (2001). "Proteins in organic solvents", Elsevier, 11:761–764.

[25] Bao, Q., Lou, Y., Xing, T. and Chen, J., (2013). "Rapid synthesis of zeolitic imidazolate framework-8 (ZIF-8) in aqueous solution via microwave irradiation", Inorganic Chemistry Communications, 37:170-173.

[26] Djaja, N. F., Montja, D. A. and Saleh, R., (2012). "The Effect of Co Incorporation into ZnO Nanoparticles", Advances in Materials Physics and Chemistry, 3:33-41.

[27] Xu, S., Zhang, H., Yu, F., Zhao, X. and Wang, Y., (2018). "Ethanol recovery of PDMS mixed matrix membranes with hydrophobically modified ZIF-90", Separation and Purification Technology, 206:80-89.

[28] The University of Texas at Dallas, Infrared Spectroscopy (IR), https://personal.utdallas.edu/~scortes/ochem/OChem_Lab1/recit_notes/ir_presentation.pdf, 9 May 2019.

[29] IR Spectrum Table & Chart, IR Spectrum Table by Frequency Range, https://www.sigmaaldrich.com/technical-documents/articles/biology/ir spectrum-table.html, 9 May 2019.

[30] Kumar, P., Bansal, V., Paul, A. K., Bharadwaj, L. M., Deep, A. and Kim, K-H., (2016). "Biological applications of zinc imidazole framework through protein encapsulation", Applied Nanoscience, 6:951-957.

[31] Feng, D., Liu, T.-F., Su, J., Bosch, M., Wei, Z., Wan, W., Yuan, D., Chen, Y-P., Wang, X., Wang, K., Lian, X., Gu, Z.-Y., Park, J., Zou, X. and Zhou, H.-C., (2014), "Stable metal-organic frameworks containing single-molecule traps for enzyme encapsulation", Nature Communications, 6:5979.

[32] Cravillon, J., Schröder, C. A., Bux, H., Rothkirch, H., Caro, J. and Wiebcke, M., (2012), "Formate modulated solvothermal synthesis of ZIF-8 investigated using time-resolved in situ X-ray diffraction and scanning electron microscopy", Royal Society of Chemistry, 14:492–498.

APPENDIX-A

SYNTHESIS CONDITIONS OF ZIF SAMPLES

Table A. 1 The amount of starting materials used for synthesis of ZIF-90 samples and HRP-ZIF-90 composites

	Solution	Weight	Concentration
R90	Zinc nitrate hexahydrate	185.6 mg/1.5 mL water	416 mM
	PVP	25 mg	50 mM
	ICA	249 mg/12.5 mL water	199 mM
R90-2	Zinc nitrate hexahydrate	185.5 mg/1.5 mL water	416 mM
	PVP	250 mg	500 mM
	ICA	240 mg/12.5 mL water	199 mM
R90-025H1	Zinc nitrate hexahydrate	44.6 mg/1.5 mL water	100 mM
	PVP	250 mg	500 mM
	ICA	480.45 mg/12.5 mL water	400 mM
	HRP	1 mg/mL PBS (1mL)	1 mg/mL
R90-2H10	Zinc nitrate hexahydrate	185.5 mg/1.5 mL water	416 mM
	PVP	250 mg	500 mM
	ICA	240 mg/12.5 mL water	199 mM
	HRP	10 mg/mL PBS (2mL)	10 mg/mL
R90-1H10	Zinc nitrate hexahydrate	185.5 mg/3 mL water	208 mM
	PVP	288 mg	500 mM
	ICA	240 mg/14 mL water	178 mM
	HRP	10 mg/mL PBS (2mL)	10 mg/mL

Table A. 2 The amount of starting materials used for synthesis of ZIF-8 samples and HRP-ZIF-8 composites

	Solution	Weight	Concentration
R8-2	Zinc nitrate hexahydrate HmIm	185.6 mg/1.5 mL water 205 mg/12.5 mL water	416 mM 199 mM
R8-025	Zinc nitrate hexahydrate HmIm	377.3 mg/4 mL water 4.1 g/40 mL water	312 mM 1.25 M
R8-025H1	Zinc nitrate hexahydrate HmIm HRP	0.178 g/2 mL water 1.970 g/20 mL water 1 mg/mL PBS (1mL)	300 mM 1.2 M 1 mg/mL
R8-025H10	Zinc nitrate hexahydrate HmIm HRP	0.186 g/2 mL water 2.05 g/20 mL water 10 mg/ml PBS (2mL)	312 mM 1.25 M 10 mg/mL
R8-05H10	Zinc nitrate hexahydrate HmIm HRP	0.186 g/2 mL water 1.025 g/20 mL water 10 mg/ml PBS (2mL)	312 mM 624 mM 10 mg/mL

APPENDIX-B

ABSORBANCE VALUES AT DIFFERENT ABTS CONCENTRATIONS

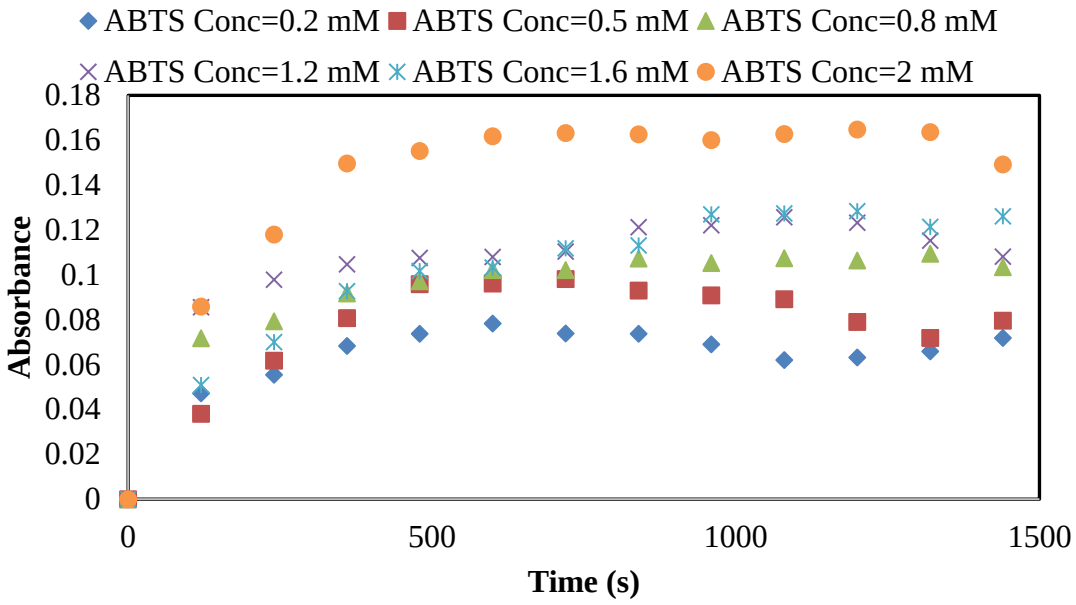


Figure B. 1 Absorbance values for R90-2H10 at different initial ABTS concentrations

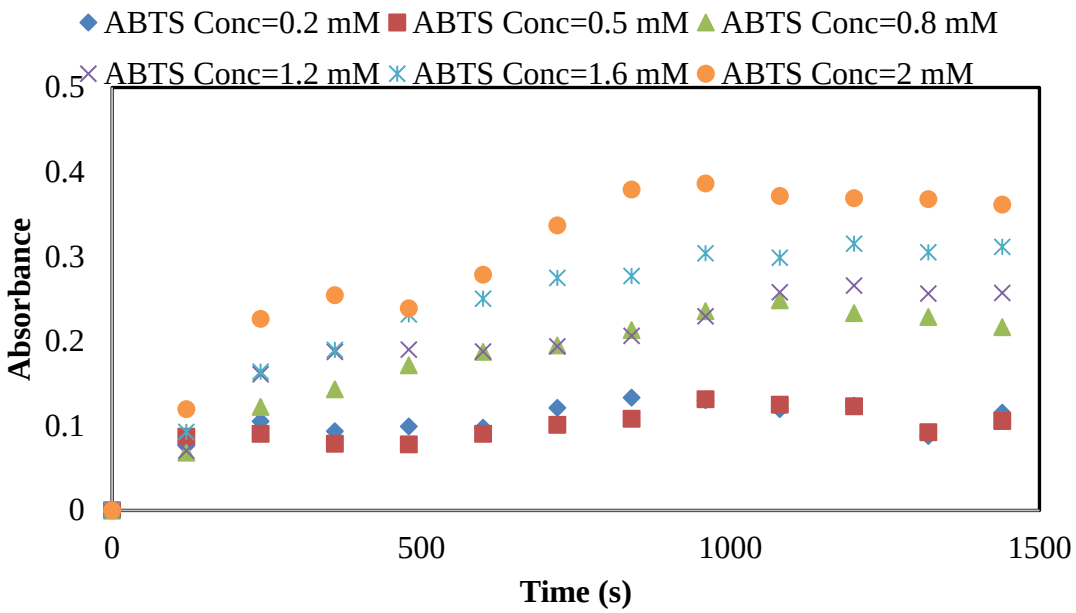


Figure B. 2 Absorbance values for R8-025H10 with different ABTS concentrations

APPENDIX-C

CALIBRATION CURVES

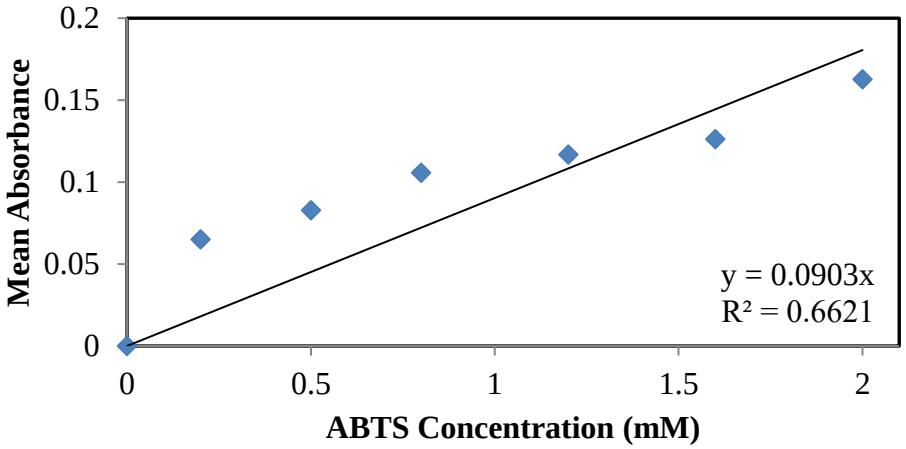


Figure C.1 Calibration curve for R90-2H10

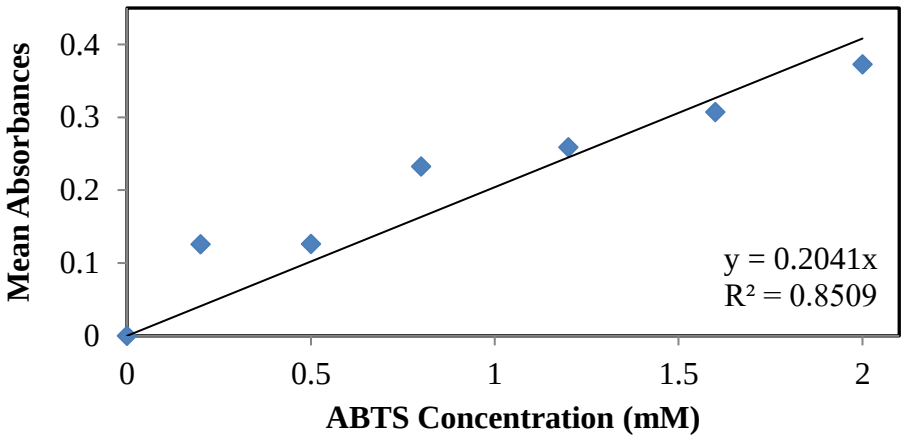


Figure C.2 Calibration curve for R8-025H10

APPENDIX-D

PRODUCT CONCENTRATION - TIME GRAPHS

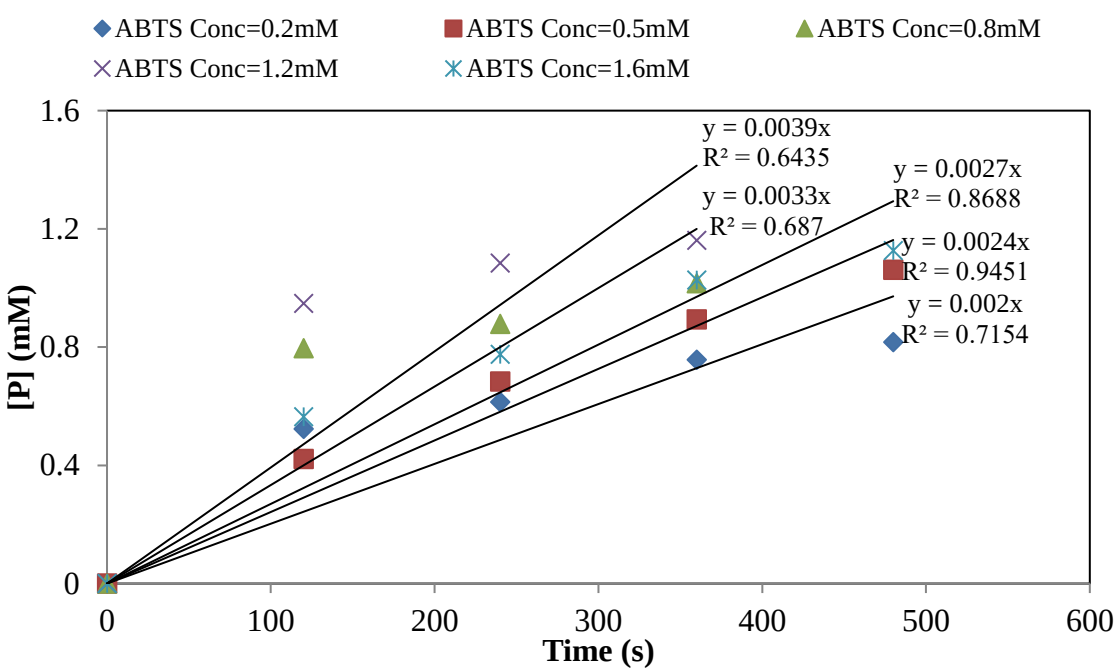


Figure D.1 Product concentration against time plot for R90-2H10

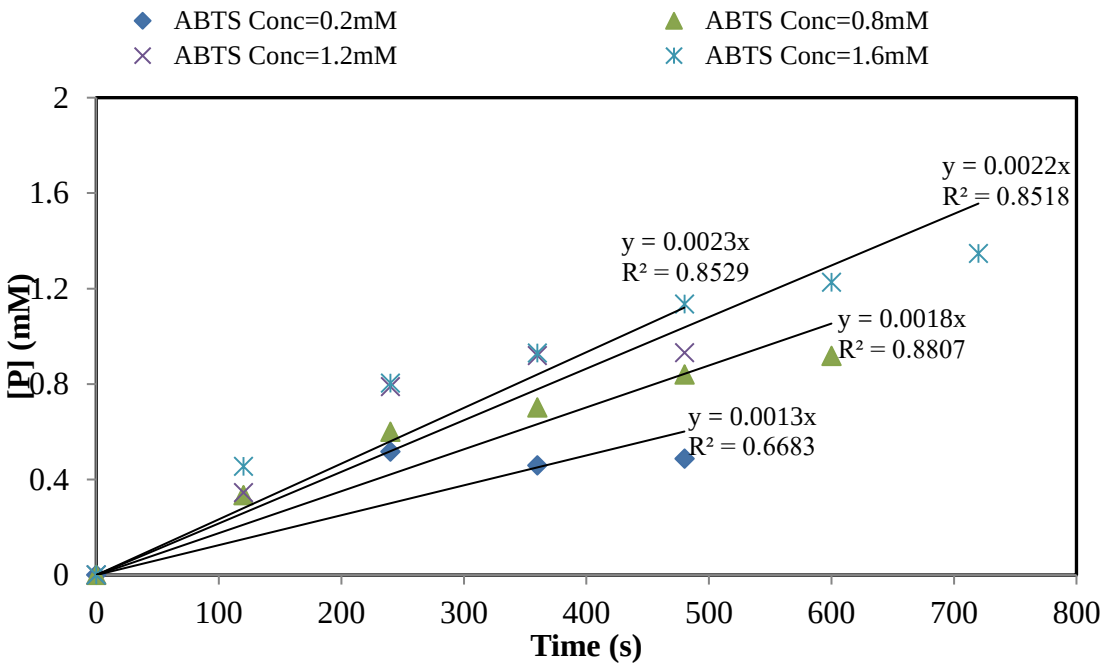


Figure D.2 Product concentration against time plot for R8-025H10

CURRICULUM VITAE

PERSONAL INFORMATION

Name Surname : Gizem GÜNER

Date of birth and place : 27.02.1992 / Ankara

Foreign Languages : English, German

E-mail : gizemguner0@gmail.com

EDUCATION

Degree	Department	University	Date of Graduation
Master	Chemical Engineering	YTU	2019
Undergraduate	Chemical Engineering	YTU	2015
High School	Science	Korfez Oruc Reis Anatolian High School	2010

WORK EXPERIENCE

Year	Corporation/Institute	Enrollment
2019-present	Endemix Natural Ingredients	R&D Assistant Specialist
2018-2019	Karlsruher Institut fur Technologie	Scientific Assistant
2017-2017	Karlsruher Institut fur Technologie	Erasmus Intern

2014-2014	Hayat Kimya Sanayi A.Ş.	Production Intern
2013-2013	Hayat Kimya Sanayi A.Ş.	Quality Assurance Intern

PUBLISHMENTS

Conference Papers

1. Güner, G., Duranoğlu, D., Kirschhöfer, F., Brenner-Weiß, G. and Franzreb, M., "Enzyme Immobilization within Metal Organic Framework for Bioassay Applications", DECHEMA 28th ATC 2019: Industrial Inorganic Chemistry – Materials and Processes, 21-22 February 2019, Frankfurt am Main, Germany.